processes

MDPI

Review

Low-Temperature Atmospheric Pressure Plasma Processes for the Deposition of Nanocomposite Coatings

Antonella Uricchio [1] and Fiorenza Fanelli [2,*]

[1] Department of Chemistry, University of Bari 'Aldo Moro', Via Orabona 4, 70125 Bari, Italy; antonella.uricchio@uniba.it
[2] Institute of Nanotechnology (NANOTEC), National Research Council (CNR), c/o Department of Chemistry, University of Bari 'Aldo Moro', Via Orabona 4, 70125 Bari, Italy
* Correspondence: fiorenza.fanelli@cnr.it; Tel.: +39-080-5442227

Abstract: Low-temperature atmospheric pressure (AP) plasma technologies have recently proven to offer a range of interesting opportunities for the preparation of a variety of nanocomposite (NC) coatings with different chemical compositions, structures, and morphologies. Since the late 2000s, numerous strategies have been implemented for the deposition of this intriguing class of coatings by using both direct and remote AP plasma sources. Interestingly, considerable progress has been made in the development of aerosol-assisted deposition processes in which the use of either precursor solutions or nanoparticle dispersions in aerosol form allows greatly widening the range of constituents that can be combined in the plasma-deposited NC films. This review summarizes the research published on this topic so far and, specifically, aims to present a concise survey of the developed plasma processes, with particular focus on their optimization as well as on the structural and functional properties of the NC coatings to which they provide access. Current challenges and opportunities are also briefly discussed to give an outlook on possible future research directions.

Keywords: nanocomposite coatings; thin film deposition; atmospheric pressure plasma; low-temperature plasma; plasma-enhanced chemical vapor deposition; aerosol-assisted plasma deposition; surface modification; organic-inorganic nanocomposite films

Citation: Uricchio, A.; Fanelli, F. Low-Temperature Atmospheric Pressure Plasma Processes for the Deposition of Nanocomposite Coatings. *Processes* **2021**, *9*, 2069. https://doi.org/10.3390/pr9112069

Academic Editor: Kosmas Ellinas

Received: 29 October 2021
Accepted: 15 November 2021
Published: 18 November 2021

1. Introduction

Low-temperature atmospheric pressure plasmas (APPs), also referred to as non-equilibrium or cold atmospheric pressure plasmas, have been studied extensively over the last decades. By providing unique reactive environments at moderate gas temperatures and atmospheric pressure, they have opened unprecedented opportunities for plasma science and technology in numerous applicative fields, such as surface engineering and nanomaterials fabrication [1–7], chemical synthesis and catalysis [8–15], environmental protection and remediation [8,14,16,17], medicine and healthcare [18–20], and food and agriculture [16,21–23].

Developing new low-temperature plasma technologies for the surface modification of materials at atmospheric pressure (AP) has attracted more and more attention in academic and industrial communities since the 1990s. Over the years, different plasma generation methods have been therefore exploited to address the rapidly increasing demand for new APP processes in surface engineering applications. They primarily include dielectric barrier discharges (DBDs), corona discharges (CDs), microplasmas (MPs), radiofrequency (RF), and microwave (MW)-driven plasmas [24–29]. As a result, a variety of APP sources are available today, offering a wide range of options in terms of sizes and geometries, plasma characteristics and regimes, electron and gas temperatures, and densities of charged and reactive species [29].

In this context, during the past two decades, significant efforts have been devoted to the development of low-temperature AP plasma reactors and processes for the preparation

of thin films [2,30,31]. Key advances have been made in the following areas: (i) the direct and remote plasma deposition of thin films, in which the substrate to be coated is located, respectively, inside and downstream the plasma generation region [2,4,30,32–34]; (ii) the preparation under open-air conditions of coatings with controlled structure and properties [2,4,34,35]; (iii) the deposition over large areas [2,36] or, oppositely, the localized or patterned deposition of functional films [4,37–39]; and (iv) the uniform coating of objects with complex geometries, including three-dimensional (3D) porous materials [4,32,40–44]. It has been demonstrated that with proper selection of the plasma source and its operating conditions as well as of the precursors nature and delivery method [2,4,45], it is possible to deposit coatings with very different characteristics in terms of chemical composition, structure, and morphology [2,4,34]. Examples in the literature range from high-quality inorganic layers (e.g., silica-like films [36,46], hydrogenated silicon nitride films [47], etc.) to polymeric coatings characterized by remarkable retention of the monomer structure [48–51] and include also a variety of nanocomposite (NC) films. These latter are defined as multicomponent layers comprising multiple different phase domains in which at least one type of the phases has at least one dimension in the nanometer range [52,53]. First studies on the low-temperature APP deposition of NC thin films were published between the end of the 2000s and the early 2010s [54–59]. Since then, numerous research groups have developed novel AP plasma-based methods for the preparation of this intriguing class of coatings [60–67]. Progress in this field has been significantly accelerated by the parallel development of aerosol-assisted plasma processes (Figure 1a) [45,68,69]. In fact, the use of aerosols of either precursors solutions or nanoparticle dispersions has allowed greatly broadening the nature and type of constituents that can be combined in the plasma-deposited NC layers.

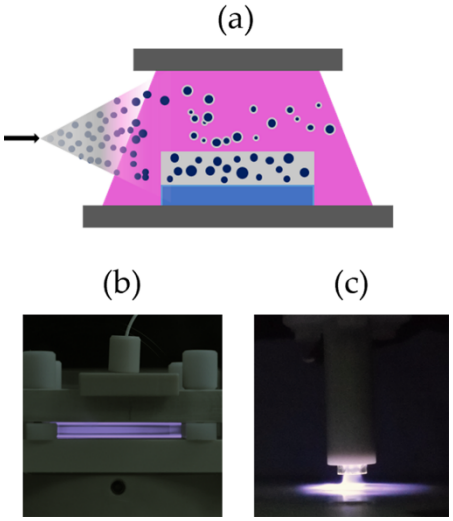

Figure 1. (**a**) Simplified scheme of an aerosol-assisted AP plasma process used for the deposition of nanocomposite coatings. (**b**) Picture of a classical dielectric barrier discharge (DBD) system used for the direct deposition of thin films at atmospheric pressure. (**c**) Picture of an AP plasma jet with DBD configuration used for the remote deposition of thin films.

Overall, to date, through rational design of the plasma sources and deposition strategies, it has been possible to explore the preparation of NC coatings with a wide range of chemical compositions (i.e., all-inorganic, all-organic, and organic-inorganic NC coatings). Low-temperature APPs have enabled, for example, the preparation of various hybrid organic-inorganic coatings consisting of inorganic nanoobjects (e.g., metal, metal oxide, salt nanoparticles) and a plasma-polymerized organic component [54–58,60,61,64,67]. Moreover, they have provided access to a unique class of biocomposite layers consist-

ing of bioactive molecules (e.g., proteins and drugs) spatially confined within nanosized domains [45,70].

Our goal with the present paper is to provide an overview of the advances that have been made since the late 2000s in the deposition of nanocomposite coatings by low-temperature AP plasmas. First, a concise survey of APP technologies and configurations used in this applicative field is presented (Section 2) to facilitate the understanding of the sections to follow. Then, the APP processes used for the deposition of NC coatings are outlined and discussed, with particular attention to their implementation and optimization using both direct and remote plasma sources (Figure 1b,c). Specifically, Section 3 addresses plasma-enhanced chemical vapor deposition (PECVD) processes, in which the vapors of one or two precursors are injected in the plasma to synthesize the NC films in a single step. Section 4 is dedicated to emerging aerosol-assisted plasma deposition (AAPD) strategies in which at least one precursor of the NC film is delivered in aerosol form. In Section 5, we review the most common functional properties and possible applications of the NC films deposited by APPs. Finally, challenges and future research perspectives are briefly outlined (Section 6).

2. Low-Temperature APP Technologies for NC Coatings Deposition

This section provides a concise survey of low-temperature APP technologies currently in use for the preparation of NC coatings. It is worth specifying that a number of recent reviews have comprehensively covered both fundamentals and material science applications of low-temperature (non-equilibrium or cold) plasmas generated at atmospheric pressure [1,2,4,24,26–28,30]. Therefore, in this section, basic concepts regarding the most used AP plasma generation methods, apparatuses, and processes are only briefly outlined to facilitate the reading of the following sections.

In the last two decades, low-temperature APPs have received great attention from both the academic and industrial communities. They have proven to be effective and versatile tools to modify the surface of a great variety of materials without affecting their bulk properties since they provide highly reactive environments close to room temperature and at atmospheric pressure. Non-equilibrium APP processes relevant to surface modification can be broadly classified into three main types:

1. Plasma deposition enables the preparation of organic, inorganic, and hybrid organic-inorganic thin films with thickness ranging from a few nanometers to a few tens of microns. The most used methods for thin film deposition with APPs are the plasma-enhanced chemical vapor deposition (PECVD) and the aerosol-assisted plasma deposition (AAPD) [2,4,31].
2. Plasma etching consists of the ablation of the substrate material through reaction with plasma-generated species to form volatile products [4,71]. It can be also exploited for removal of surface contaminants (i.e., plasma cleaning) [4,72].
3. Plasma treatment consists of the modification of the topmost layers of the substrate through, for example, grafting of specific chemical groups, variation of the crosslinking degree, and change of the surface morphology [4,73,74].

Undoubtedly, the main motivation to investigate APP technologies has lied in the advantages offered by the atmospheric pressure operation. First of all, the absence of vacuum equipment can lead to significant reduction in the cost of plasma reactors while simplifying their maintenance and handling. It can also enable plasma processing in open-air conditions and facilitate the integration of plasma apparatuses in continuous production lines. Another important advantage associated with AP operation resides in the possibility of igniting the plasma into millimeter and submillimeter gaps and cavities [1,4,26,42]. This definitely makes the modification of the inner surfaces of tubes, channels, and porous materials (e.g., scaffolds, foams, etc.) more feasible [40–43,75]. AP operation is also more compatible with the processing of highly-outgassing materials [76] as well as with the use of liquid aerosols [2,45,68,69]. Interestingly, it provides unique access to the plasma-assisted synthesis and processing of nanomaterials in liquids [1,3,7,77–79].

The above-discussed advantages render AP plasmas an attractive alternative to low-pressure (LP) plasmas. However, at present, the general consensus seems to be that it will be hardly possible for AP plasma technologies to replace LP ones in surface engineering applications where, for instance, a very precise control of the reactive atmosphere, ion bombardment, and thin film growth is strictly required (e.g., microelectronics, optics).

Since the late 1990s, different types of non-equilibrium APPs have been exploited in surface engineering to meet the growing demand for new plasma processes at atmospheric pressure. As a consequence, many different plasma sources have been devised and currently offer a wide range of possibilities in terms of configurations and sizes, plasma characteristics and regimes, electron and gas temperatures, etc. [4,24,26,27,29]. For example, Figure 2 reports some representative APP systems used for the deposition of NC coatings.

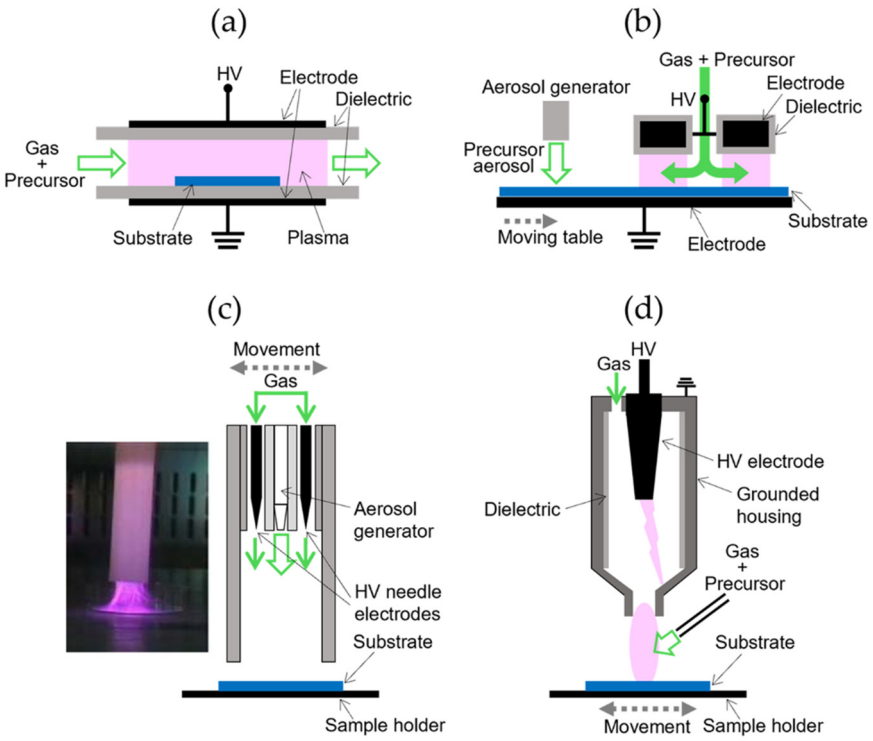

Figure 2. Selected examples of APP systems used for the preparation of nanocomposite coatings. (**a**) Classical symmetric parallel-plate DBD system [60,62,64] used for the direct PECVD or AAPD of NC films. (**b**) Parallel-plate DBD system used in [59,80] for NC film deposition from aerosols of NPs dispersions or precursors solution. (**c**) Corona discharge-based plasma jet (PlasmaStream™) used for remote AAPD processes [57,81,82]. Reproduced with permission from [81]. (**d**) Arc jet commercialized by Plasmatreat used for the remote AAPD [83] or PECVD [84] of NC films.

To better understand the architecture of these systems, it is important to keep in mind that the plasma surface modification of materials can be carried out by using two main approaches. In the first approach, referred to as direct approach, the substrate is placed in the plasma generation region between the electrodes and is therefore directly exposed to the plasma [2] (Figures 1b and 2a,b). Differently, in the second approach, known as remote approach, the substrate is located downstream of the plasma generation region [30]. At atmospheric pressure, this latter approach is typically associated with the use of plasma jets or torches (Figures 1c and 2c,d) [4], i.e., remote plasma sources in which the plasma is generated remotely within the device and launched in the external environment in the form of a so-called "plasma plume" towards the substrate to be treated. APP jets give the possibility of placing the substrate outside the physical boundaries of the plasma source. Consequently, they are particularly suited for the processing of com-

plex 3D objects, for the localized surface modification, and for the integration in existing production lines [4,39,43,71,73,74,85,86]. It is also worth noting that, as shown, for example, in Figure 2b–d, APP apparatuses are very often equipped with sample/plasma source movement systems, which allow considerably enlarging the treated area and improving the homogeneity of the surface modification (e.g., motorized sample-holders, roll-to-roll system, multi-axis robotic arms for controlled motion of the plasma source, etc.) [1,4,43,56,66,74,87].

By examining the literature, it appears that the types of AP plasmas used for the preparation of NC films primarily include dielectric barrier discharges, corona discharges, and a range of arc-based plasma jets:

- Dielectric barrier discharges (DBDs) are generated using electrode configurations containing at least a dielectric layer between the electrodes [24,28]. The dielectric material prevents arc transition and allows achieving non-equilibrium plasma conditions at atmospheric pressure. DBDs are mostly operated with alternating (AC) high voltages at frequencies between 50 Hz and a few hundreds of kHz [24,28]. However, recently, the use of pulsed or radiofrequency power supplies (i.e., frequency equal or greater than 1 MHz) is attracting growing interest [28,88]. Over the years, DBDs have become very popular in surface processing due to their versatility and scalability [2,4,32,89,90]. They can be generated by using a variety of electrode configurations (e.g., parallel-plate, coaxial cylindrical, coplanar electrode arrangements, etc. [24,28]) that can be implemented for both direct and remote surface processing [2,4]. For example, Figure 2a,b shows two different types of parallel-plate electrode systems. The first presents a classical symmetric geometry (i.e., assembly of two identical electrodes both covered by a dielectric layer, Figure 2a) and has been widely exploited for the direct deposition of thin films (e.g., NC films [60,62,64,65,68,89]) as well as for various plasma treatments and etching processes [89]. The second is manly used for thin film deposition (Figure 2b): it consists of two flat, parallel high-voltage (HV) electrodes covered by a dielectric plate and a moving stage as grounded electrode [59,80].
- Corona discharges (CDs) are produced in the close proximity of pin or thin wire HV electrodes due to electric field enhancement [24,29]. They are commonly generated by using both DC and AC power supplies (operating in continuous or pulsed mode) at voltages up to several tens of kV [24,29]. The vast literature on the use of CDs in surface engineering includes, among others, recent studies dealing with the direct and remote deposition of NC coatings [57,61,63,91]. Figure 2c shows the schematic diagram of the PlasmaStream™ system, i.e., a corona-based plasma jet specifically optimized for the open-air aerosol-assisted deposition of thin films (including NC thin films) [57,81,82]. The PlasmaStream™ system presents two needle electrodes located either side of a central aerosol generator used for precursor delivery. This arrangement is positioned at one end of a quartz or polytetrafluoroethylene (PTFE) tube in which the CD develops extending towards the substrate.
- Low temperature arc-based plasma jets or torches are currently widely used for thin films deposition and the surface treatment of both polymeric and inorganic materials [4]. In principle, arc jets are thermal plasma sources characterized by high gas temperatures. However, it has been demonstrated that they can be able to eject in the external environment a plasma characterized by relatively low gas temperature, provided that the appropriate power supply, source geometry, and operating conditions are selected [66,85,92–97]. For example, Figure 2d reports a plasma source commercialized by Plasmatreat and used for NC film deposition in [83,84].

A more limited number of papers also focuses on the preparation of NC coatings by using other types of AP plasmas, such as high-frequency plasmas and microplasmas. For example, very few works investigated the remote deposition of NC coatings with RF and MW plasma jets [98,99], in which the use of high-frequency AC electric fields is

exploited to obtain stable and uniform non-equilibrium plasmas at atmospheric pressure. Details on this class of APP jets can be found in [4,25,27,100,101].

As non-equilibrium plasmas confined within sub-millimeter cavities in at least one dimension, microplasmas (MPs) offer stable operation at atmospheric pressure, non-thermal characteristics, and high power densities. These features make them particularly suited for the synthesis of nanomaterials [1,7]. We refer readers interested in MPs and their use for nanofabrication to a number of reviews [1,4,7,26,77]. In the context of this review, it is worth mentioning that a number of studies demonstrated that microplasma-based processes can play a key role in multistep procedures used for NC films preparation. For example, microplasma jets can be used to assist the synthesis of NPs in a pre-deposited film [102,103]. Moreover, the coupling of microplasmas with liquids can lead to the synthesis in solution of nanohybrid and nanocomposites [104,105] as well as to the surface treatment of pre-synthesized NPs to improve their dispersion in the matrices of NC films [77].

3. Plasma-Enhanced Chemical Vapor Deposition of NC Coatings

Atmospheric pressure PECVD processes used for the preparation of NC thin films can be classified in single-source and dual-source approaches in which, respectively, vapors of a single or two precursors are diluted in a carrier gas (also referred to as main or dilution gas, i.e., helium, argon, nitrogen, air) and delivered to the AP plasma [2,4] to synthesize in a single step the different constituents of the NC layer. Specifically, in the plasma, the precursor molecules undergo fragmentation (for example, by collision with energetic electrons or metastable atoms/molecules of the carrier gas [2]) and consequent gas-phase and/or gas-surface reactions, which contribute to the growth of the hybrid layer.

For example, Shelemin et al. [106] investigated the direct PECVD of organic/inorganic NC films using titanium tetraisopropoxide (TTIP, $Ti[OCH(CH_3)_2]_4$) as single precursor. In particular, PECVD processes were carried out by using a parallel-plate DBD fed with nitrogen or air in mixture with TTIP vapors. When air was used as carrier gas, the deposited films consisted mainly of TiO_2 NPs because oxygen present in air acted as scavenger of the organic component. In contrast, nitrogen/TTIP feed mixtures allowed the deposition of highly porous hybrid films consisting of inorganic nitrogen-doped TiO_2 NPs wrapped by a nitrogen-rich plasma polymer (Figure 3a,b). The NC composition was controlled as a function of the PECVD conditions; for instance, the relative contribution of the inorganic component was increased by increasing the power delivered to the plasma (i.e., the input power).

Rapp et al. [84] reported the remote PECVD of inorganic SiO_x/TiO_x composite films by using an arc-based plasma jet and two different precursors, i.e., tetraethylorthosilicate (TEOS) and titanium tetraisopropoxide. The plasma source was operated with air, while the precursors vapors were simultaneously injected in the downstream region (also referred to as post-discharge region) before the source outlet nozzle (see Figure 2d). Scanning electron microscopy (SEM) observations revealed the granular structure of the films due to the presence of nanoparticles with average size of 500 nm. The deposited coatings exhibited photocatalytic and antimicrobial activity under visible light irradiation.

It is worth noticing that, overall, a very few works appeared in the literature on the use of PECVD processes for the deposition of NC coatings. This is reasonably due to the fact that the operational window of these processes is typically very limited because it is challenging to find the deposition conditions under which the contemporaneous synthesis of the different NC constituents can occur.

Interestingly, the literature offers examples in which the PECVD is included in multistep deposition procedures leading to layered NC coatings [107–113]. In their simplest form, these coatings consist of two layers, i.e., a layer of inorganic NPs overcoated with a plasma-deposited thin film that enables the NPs immobilization on the substrate [113]. The NPs layer is typically obtained from NPs dispersions via dip-coating or drop-casting procedures. For example, Reniers and coworkers [107,108] used a simple procedure wherein (i) first, an aqueous dispersion of TiO_2 or SiO_2 NPs was deposited onto silicon wafers, and (ii) then,

after solvent evaporation, the NPs were overcoated with a plasma-polymerized fluorinated layer. The PECVD process was carried out using a parallel-plate DBD fed with a noble gas (He and Ar) and an unsaturated fluorocarbon (i.e., perfluoro(2-methylpent-2-ene)). The authors investigated the effect of the amount and chemical nature of the NPs on the roughness and hydrophobic properties of the coatings as well as on the chemical stability of fluorinated overlayer.

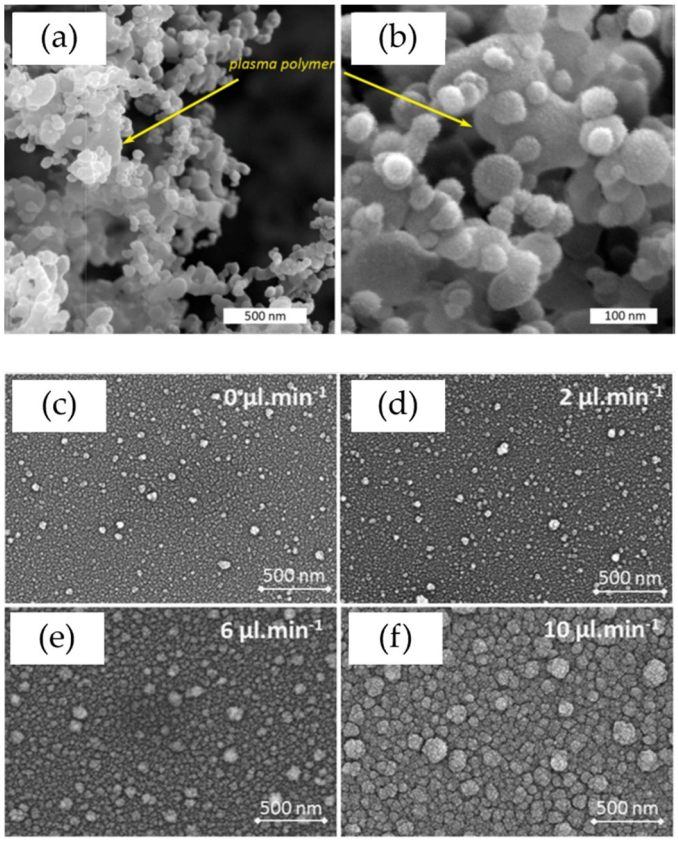

Figure 3. Scanning electron microscopy (SEM) images of different nanocomposite films deposited by AP plasma from conventional single-source or double-source precursors. (**a**,**b**) NC film consisting of inorganic nitrogen-doped TiO_2 NPs wrapped by a nitrogen-rich plasma polymer deposited by direct PECVD using a DBD fed with nitrogen and vapors of titanium tetraisopropoxide (TTIP). Reproduced with permission from [106]. (**c**–**f**) NC films consisting of crystalline TiO_2 NPs embedded into a SiO_2 matrix deposited by using an arc-jet fed with nitrogen and the aerosols of TTIP and hexamethyldisiloxane (HMDSO). SEM images refer to the NC coatings deposited by increasing the HMDSO delivery rate from 0 to 10 $\mu L \cdot min^{-1}$ and keeping constant the TTIP delivery rate (6 $\mu L \cdot min^{-1}$). Reproduced with permission from [66].

Sandwich-structured films represent another family of layered NC coatings that can be obtained, for example, by incorporating inorganic NPs between two plasma-deposited layers. The preparation of these NC coatings requires a three-step procedure, such as the one reported in [110–112]. In these studies, antibacterial non-woven polyethylene terephthalate (PET) fabrics were prepared by sandwiching inorganic nanoparticles (e.g., Ag, ZnO, or Cu NPs) between two organosilicon layers obtained by PECVD using a corona-based plasma jet fed with N_2, O_2, and an organosilicon precursor (tetramethyldisiloxane or hexamethildisiloxane). In particular, the authors optimized the following procedure: (i) first, a 70-nm thick organosilicon layer was deposited by PECVD on the fabric to control the silver nanoparticles adhesion to the PET fibers; (ii) then, NPs were deposited on the precoated fabrics by a facile dip-drying method; and (iii) finally, the NPs were covered by a second organosilicon layer (thickness of 10–50 nm) acting as barrier layer.

4. Aerosol-Assisted Plasma Deposition of NC Coatings

In the present section, we first provide a general overview of the AAPD technique and its main features (Section 4.1). Then, we review the studies that explored the AP plasma deposition of NC films from aerosols of conventional liquid precursors (Section 4.2), nanoparticle dispersions or dry particles (Section 4.3), and precursors solutions (Section 4.4). Since the use of aerosols poses new challenges in the optimization of plasma deposition processes, we discuss in detail the key parameters controlling the growth of the hybrid layers as well as specific aspects related to the use of both direct and remote plasma sources.

4.1. General Overview

Recently, the AAPD has emerged as the most promising and versatile technique to prepare NC thin films using atmospheric pressure plasmas. This is primarily due to the fact that there is no stringent requirement for volatile precursors as in case of conventional PECVD processes [114,115]. In fact, the use of aerosols can enable the delivery of low-volatility or thermally-unstable molecular precursors as well as of diverse unconventional precursors, such as, for example, a variety of nanoparticle dispersions and precursor solutions [114–116]. Interestingly, it has been also shown that AAPD can lead to greater deposition rates as compared to PECVD since aerosol delivery allows obtaining high mass-transport rates of the precursors [114,115]. It is also worth noting that the literature offers very interesting examples of both low pressure [117,118] and atmospheric pressure AAPD processes. However, it is commonly acknowledged that the use of aerosols (in particular, liquid aerosols) is more convenient and practical when coupled with AP plasmas rather than with LP ones.

Taking into account the numerous variants reported in the literature, atmospheric pressure AAPD processes used for the deposition of NC coatings can be broadly defined as single- or sequential multi-step deposition methods in which at least one precursor of the nanocomposite layer is delivered in aerosol form. It is worth specifying that this general definition also includes hybrid dual-source processes in which the NC film is deposited from an aerosolized precursor and a gaseous precursor [59,65,70,80]. Typically, the aerosolized precursors are injected directly in the plasma [54,56,60,62,64,65] during the deposition process. However, a possible alternative is to spray-deposit the precursor on the substrate surface right before plasma exposure [59,80,119] using, for example, an APP reactor with a configuration similar to the one reported in Figure 2b. In case of liquid precursors (e.g., pure liquid molecular precursors, NPs dispersions and precursors solutions), the aerosol is typically generated by pneumatic or ultrasonic atomizers (or nebulizers) [45,68,114]. Pneumatic atomizers exploit a high-velocity gas stream to break up the liquid precursor in fine droplets. The atomizing gas, which typically is the main gas used for plasma generation, also ensures the transport of the precursor mist to the plasma reactor [60,68]. In contrast, ultrasonic atomizers utilize high-frequency vibrations to convert the liquid precursor into a fine mist [114]. They can be, for example, either integrated in the discharge cell (e.g., in parallel-plate DBD systems [120]) or located upstream the plasma generation region. On the other hand, in case of solid precursors, such as dry particles, the aerosol is generated by various methods which can include the use of fluidized beds, brush mechanisms, moving toothed belts, and Venturi aspirators. These methods enable the dispersion of dry particles in a carrier gas (i.e., gas-borne particles), which also ensures their delivery to the plasma.

4.2. Deposition of NC Coatings from Conventional Liquid Precursors in Aerosol Form

NC coatings can be deposited by atmospheric pressure AAPD, first of all, from conventional single-source or dual-source precursors commonly used in PECVD (Section 4.1). In these AAPD processes, single- or two-liquid molecular precursors are atomized and delivered to the plasma. To the best of our knowledge, only one study to date has exploited this deposition strategy. In this work [66], transparent anti-fogging and self-cleaning TiO_2/SiO_2 NC films were deposited on polymer substrates by using an AP arc jet fed with

air, titanium tetraisopropoxide, and hexamethyldisiloxane (HMDSO). The proposed AAPD strategy enabled the simultaneous synthesis and embedment of anatase TiO_2 NPs into a SiO_2 matrix. In particular, it relied on the concomitant and separated injection of aerosols of TTIP and HMDSO in the downstream (or post-discharge) region of the arc-jet before its outlet. TTIP was injected into the upper part of the downstream region near to the arc generation zone, where gas phase reactions and the subsequent formation of crystalline TiO_2 NPs are promoted by the high density of excited species and the relatively high gas temperature. In contrast, HMDSO was injected into the lower part of the downstream region close to the substrate in order to promote heterogeneous chemical reactions at the substrate surface and obtain the growth of a SiO_2 layer that could embed the crystalline TiO_2 NPs. The HMDSO/TTIP delivery rate ratio was varied in order to tune the chemical composition and morphology of the nanocomposite coatings. In particular, the increase of the HMDSO delivery rate from 0 to 10 $\mu L \cdot min^{-1}$, while keeping constant the TTIP one (6 $\mu L \cdot min^{-1}$), led to a linear increase of the Si/(Si+Ti) ratio of the coatings determined by X-ray photoelectron spectroscopy (XPS), to an increase of the deposition rate from about ~0.8 to ~2.5 $\mu m \cdot min^{-1}$, as well as to the appearance of a cauliflower morphology (Figure 3c–f). Interestingly, it was shown that the separate injection of the two precursors was necessary to generate a two-phase structure and therefore to allow the synthesis of a NC layer. In fact, by injecting both precursors at the same location, a single $SiTiO_x$ phase was obtained. Overall, this study provides a very illustrative example because, on one hand, it demonstrates the effectiveness of the proposed aerosol-assisted strategy; on the other hand, it shows that, as in PECVD processes (Section 4.1), the use of conventional molecular precursors requires very careful process optimization to obtain the contemporaneous synthesis of the constituent phases of the NC. This explains why an increasing number of studies has been recently published on the use of aerosolized unconventional precursors, such as nanoparticle dispersions, in liquid solvents (Section 4.3), dry particles (Section 4.3), and solutions (Section 4.4).

4.3. Deposition of NC Coatings from Aerosols of Either Nanoparticle Dispersions or Dry Particles

4.3.1. Aerosols of Nanoparticle Dispersions

A number of pioneering papers published between the late 2000s and the early 2010s [54–59] successfully explored the possibility of combining the aerosol of a NPs dispersion with a low-temperature AP plasma as a viable route to prepare NPs-containing NC coatings. This strategy was inspired by the literature on the preparation of nanostructured and nanocomposite materials by aerosol-assisted methods, such as spray-deposition and aerosol-assisted CVD [60,68,114–116,121–123]. Since then, an increasing number of studies has been carried out on a variety of direct and remote AAPD processes in which a dispersion of preformed inorganic NPs in a proper solvent is atomized and injected in the AP plasma together with, if necessary, an additional gaseous or aerosolized molecular precursor. These processes enable the single-step deposition at atmospheric pressure and room temperature of all-inorganic [62,76] or organic-inorganic [60,64] NC coatings in which the preformed inorganic NPs are embedded in an inorganic or polymer matrix formed through the so-called plasma polymerization of the dispersion solvent and/or of the additional precursor. Typically, the composition and crystallinity of the inorganic NPs injected in the plasma and incorporated in the coating is not affected by the deposition process [60,62,64,124,125]. In contrast, the chemical composition of the NC matrix (i.e., inorganic or polymer matrix) depends on several factors including the chemical nature of the dispersion solvent and/or of the additional precursor, the presence of reactive additives (e.g., oxygen), as well as the plasma generation conditions (e.g., input power). The use of inorganic NPs dispersions in AAPD processes presents two main advantages. The first is that, in principle, a large variety of preformed nanoobjects (e.g., metal NPs [55], inorganic oxides NPs [54,57,60,68], graphene nanosheets [67], etc.) can be injected in the plasma and incorporated in the coating. The second resides in the fact that, since preformed NPs are utilized, these processes have not to fulfill the requirements for the in-situ synthesis of

the NPs as well as for the control of their size, shape, and properties. However, in spite of these advantages, a critical issue to address is the preparation of stable NPs dispersions. In fact, it is important to achieve a good dispersibility of the inorganic NPs in the selected solvent in order to avoid excessive agglomeration phenomena. For instance, two different methods have been proposed to prepare stable inorganic NPs dispersions in liquid organic precursors (e.g., hydrocarbons, organosilicon compounds). The first involves the surface functionalization of the nanoparticles with a capping agent (e.g., a surfactant). For example, Fanelli et al. [60] functionalized the surface of commercial ZnO NPs with oleate (i.e., a surfactant with a long alkyl chain) using a simple wet chemistry procedure to obtain stable dispersions in hydrocarbon solvents. The second exploits the addition to the dispersion of a noncovalent compatibilizer [54,57,62]. For instance, Bardon et al. [54] added small amounts of ethanol (3%) to dispersions of aluminium-cerium oxide ($AlCeO_3$) NPs in hexamethyldisiloxane to improve the NPs dispersibility in the liquid organosilicon precursor.

Several studies revealed that the atmospheric pressure AAPD from aerosols of NPs dispersions typically leads to NC coatings containing quasi-spherical NPs agglomerates with size ranging between a few hundred nanometers and a few micrometers (Figure 4a,b) [57,60,62,64,76,124–130]. The NC matrix covers the NPs agglomerates to an extent depending on the matrix growth rate, allows their immobilization in the coating, and ensures the coating adhesion to the supporting substrate [60,124–126,129]. The NPs agglomerates can form as a result of (i) a primary agglomeration that can occur in the dispersion and can be rather severe depending on the nature of the NPs and of the solvent [54,130] and (ii) a secondary agglomeration that can take place after dispersion atomization due to solvent evaporation (Figure 4a,b) [60,130]. The experimental evidences support the hypothesis that a certain solvent evaporation occurs at the aerosol droplets surface, and therefore, the NPs undergo evaporation-induced agglomeration to form closely packed quasi-spherical structures (Figure 4a,b) [60,121–123,130]. Interestingly, the formation of analogous NPs agglomerates is widely reported in the literature on aerosol-assisted processes involving the atomization of NPs dispersions [68,121–123].

There is no doubt that, among others, the major challenge to address when depositing NC films from APPs fed with an aerosolized NPs dispersion is to obtain NC coatings with the desired chemical composition and morphology. This requires a fine control of the film growth and, more specifically, of the co-deposition of the NPs and the matrix. In the following, we present advances that have been recently made in the understanding of the influence of various process parameters when both direct and remote plasma sources are used. In particular, we discuss separately studies dealing with direct and remote deposition approaches in order to better enlighten specific aspects related to their optimization.

The most common direct AAPD methods involve the use of a parallel-plate dielectric barrier discharge fed with a main gas and the aerosol of dispersion of inorganic NPs in an organic solvent, which acts as precursor of the NC matrix. Such methods are, in principle, very facile and convenient. However, a detailed understanding of the different factors that influence the growth of the matrix and the NPs transport to the surface is needed to properly control the NPs-to-matrix ratio in the NC.

As far as the matrix is concerned, it is important to take into account that the precursor polymerization rate in the plasma (and, in turn, the matrix growth rate) depends on both the reactivity of the precursor [124] and the DBD power (which increases with both the excitation frequency and the applied voltage) [128]. It is worth specifying that the greater the power, the higher the density of energetic species able to activate the matrix precursor and thus the greater the matrix growth rate.

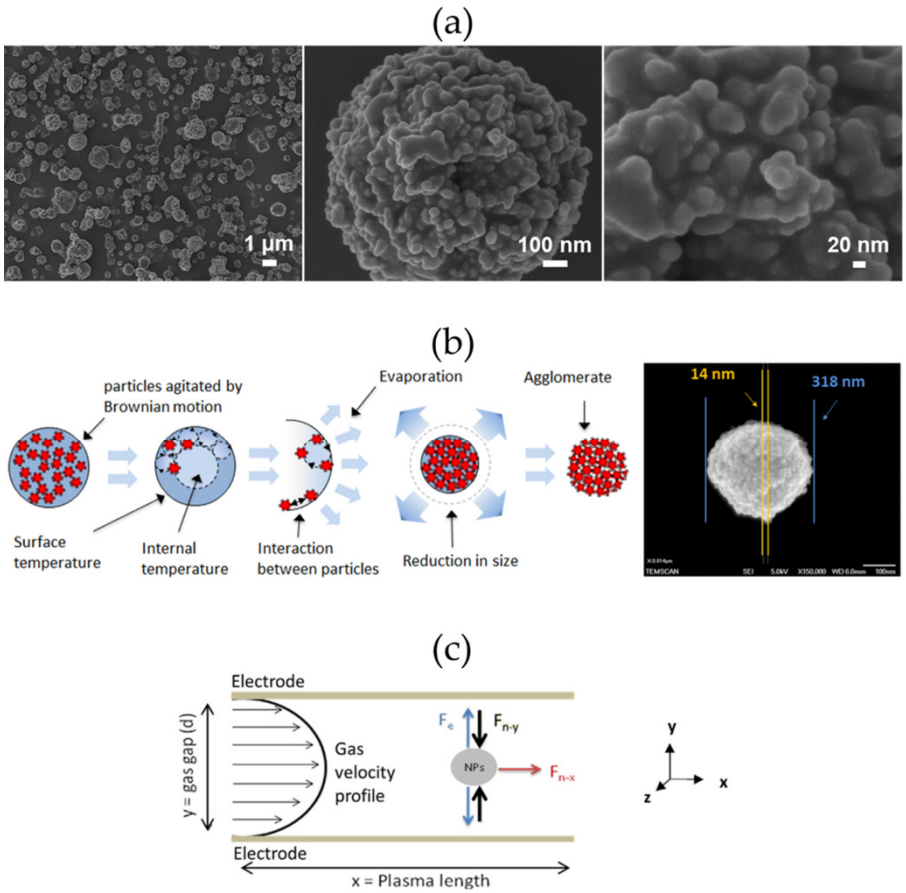

Figure 4. (**a**) Representative SEM images of a hydrocarbon polymer/ZnO NPs nanocomposite coating deposited for 10 min in a parallel-plate DBD fed with He and the aerosol of dispersion of oleate-capped ZnO NPs in n-octane. Reproduced with permission from [60]. (**b**) Schematic of the nebulization process explaining NPs agglomeration and SEM image of a NPs aggregate collected after atomization of a NPs dispersion. Reproduced with permission from [130]. (**c**) Schematic representation of the gas flow profile between the electrodes of a parallel-plate DBD system, and of the forces considered in [64] for the calculation of the NPs trajectory: F_e is the electrostatic force, $F_{n\text{-}x}$ is the neutral drag force along the x-axis, $F_{n\text{-}y}$ is the neutral drag force along the y-axis. Reproduced with permission from [64].

A more detailed discussion is needed to explain the key factors that influence the NPs deposition. Studies by Profili et al. [130,131] and Brunet et al. [64,127,128] focused on understanding and controlling the trajectory of NPs across the DBD as well as their transport to the surface. It is well-known that the NPs transport in the plasma can be governed by five forces which include the gravity (F_g), neutral drag (F_n), ion drag (F_i), thermophoresis (F_{th}), and electrostatic (F_e) forces [64,127,131]. The last three forces are related to the plasma characteristics: the ion drag force is controlled by the ion density according to the discharge regime; the thermophoresis force is related to the temperature gradients between the gas bulk and the electrodes or between different plasma regions; and the electrostatic force is proportional to the NPs charging (which linearly increases with the NPs radius) and to the electric field [64,127]. According to the simplified model proposed in [64,131], the NPs transport in the DBDs used for NC film deposition is mainly governed by the electrostatic force and the neutral drag forces (Figure 4c). In fact, since in the DBD the neutral species temperature is close to the room temperature, and the ionization degree is very low, the thermophoresis and ion drag forces can be considered negligible as compared to the electrostatic and neutral drag forces (Figure 4c). In addition, experimental evidences demonstrated that the gravity force does not play a significant role in favoring the NPs

collection on the substrate surface as compared to the electrostatic force (Fe) even with the discharge off [130]. As a consequence, the following two considerations can be made regarding the transport of the NPs and NPs agglomerates in the DBD:

- Since in the parallel-plate DBD, the gas flow is laminar, the gas velocity profile is parabolic, as shown in Figure 4c. Therefore, the NPs are more likely to be located at the center of the discharge gap. However, the sinusoidal voltage applied to the electrodes to generate the plasma is able to induce an oscillation of the particles. This explains why the voltage frequency needs to be sufficiently low to obtain an oscillation amplitude large enough to allow the NPs to reach the substrate surface [64].
- By increasing the gas flow rate, it is possible to transport the NPs farther and farther from the entrance in the DBD cell. As a consequence, the greater the gas flow rate, the more uniform the NPs deposition over the entire electrode area and thus the more spatially homogeneous the coatings [127].

The above discussion about the fundamental mechanisms that control the growth of the matrix and the transport of the NPs to the substrate surface can facilitate the understanding of the studies which explored the influence of various process parameters on the chemical composition and morphology of the deposited coatings. These studies can be divided into two classes: the first investigated the influence of the composition of the starting NPs dispersion [32,60,124,125,132]; and the second explored the effect of the electrical conditions used to generate and sustain the DBD [62,64,128,129,133].

The influence of the composition of the starting dispersion was investigated by varying both the NPs concentration and the composition of the solvent mixture [32,60,124,125,132]. For example, Fanelli et al. [60] carried out a comprehensive study on the properties of hydrocarbon polymer/ZnO nanoparticles NC coatings deposited on flat glass samples by using a DBD fed with helium and the aerosol of a dispersion of oleate-capped ZnO NPs in n-octane. As summarized in Figure 5a, it was demonstrated that the increase of the NPs concentration in the starting dispersion (0.5–5 wt%) has a significant effect on the chemical composition and morphology of the NC films. In fact, it promotes a remarkable increase of the ZnO NPs content in the coating and, consequently, induces a transition from a polymer-dominated smooth morphology to a nanoparticles-dominated rough surface morphology (see cross-sectional SEM images in Figure 5a). Interestingly, it is possible to obtain superhydrophobic coatings (advancing and receding water contact angles > 160°) with low-contact-angle hysteresis (<10°). This wettability behavior derives from the synergistic effect of the hierarchical multiscale surface texture due to NPs incorporation and the low surface energy of the hydrocarbon polymer. In a subsequent work [124], dispersions of oleate-capped ZnO nanoparticles (NPs) in binary n-octane/1,7-octadiene solvent mixtures were used. It was found that 1,7-octadiene addition is able to trigger the growth of the organic and inorganic components of the NC coating due to the high reactivity conferred by the two terminal carbon-carbon double bonds. In particular, as reported in Figure 5b, when the concentration of 1,7-octadiene in the hydrocarbon mixture is very low (0.5–2 vol%), the immobilization of NPs agglomerates on the substrate surface is promoted; in contrast, at greater concentration of octadiene (>2 vol%), the growth of the organic component is favored.

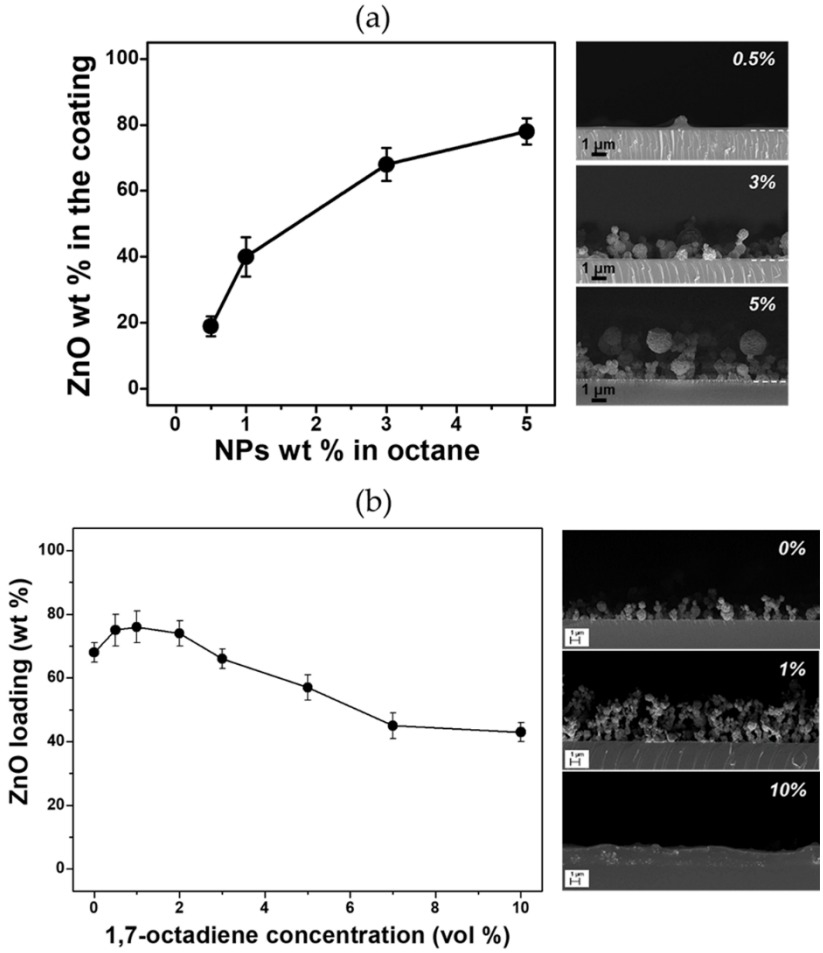

Figure 5. Effect of the composition of the starting NPs dispersion on the chemical composition and morphology of hydrocarbon polymer/ZnO NPs NC coatings deposited in a parallel-plate DBD fed with He and the aerosol of dispersion of oleate-capped ZnO NPs in hydrocarbon precursors. (**a**) ZnO loading and cross-sectional SEM images of NC coatings deposited from dispersions at different concentration of the oleate-capped ZnO NPs in n-octane (0–5 wt%). Reproduced with permission from [60]. (**b**) ZnO loading and cross-sectional SEM images of coatings deposited from dispersions characterized by different concentrations of 1,7-octadiene in the n-octane/1,7-octadiene solvent mixture. Reproduced with permission from [124].

A number of recent studies demonstrated the possibility of tuning the properties of the NC coatings by simply varying the electrical parameters utilized for DBD generation, such as the excitation frequency [62,64], the waveform [62,128,129] and the amplitude [133] of the voltage applied to the electrodes. In particular, the works by the Massines [64,128,129] and Gherardi groups [62] on the influence of the excitation frequency, the applied voltage waveform, and the modulation mode are of great conceptual importance. In [64], Massines and coworkers investigated the impact of the excitation frequency on the properties of organic-inorganic NC films deposited in a DBD fed with argon and dispersions of TiO_2 NPs in isopropanol (i.e., isopropyl alcohol, IPA). Results revealed that, at low frequency (1–10 kHz) (Figure 6a), the transport of NPs to the surface is favored due to the electrostatic force and dominates over isopropanol plasma polymerization. In contrast, by increasing the frequency from 10 to 50 kHz (Figure 6a), the growth rate of the organic component increases because of the increase of the plasma power, while the NPs remain mainly trapped in the gas phase because their oscillation amplitude is reduced. In a subsequent publication [128], the same group demonstrated the possibility to achieve a fine control of the nanocomposite thin film composition by simply alternating two excitation frequencies through a frequency shift keying (FSK) double modulation. As shown in

Figure 6b, this modulation mode consists of periodically alternating sinusoidal voltages at two frequencies, i.e., a low frequency (LF, e.g., 1 kHz) and a high frequency (HF, e.g., 15 kHz), the period of the FSK waveform (T_{FSK}) being the sum of the LF time (T_{LF}) and the HF time (T_{HF}). In particular, the LF voltage is used for transporting NPs to the surface, while the HF voltage is used to boost the growth rate of the organic component. Interestingly, it was demonstrated that by simply changing the duty cycle (DC), defined as T_{HF}/T_{FSK}, it is possible to achieve fine control of the NPs/matrix ratio in the NC coating. Interestingly, in another study, Profili et al. [62] investigated the growth dynamics of TiO_2-SiO_2 NC coatings in a parallel plate DBD using nebulized TiO_2 NPs dispersions in hexamethyldisiloxane. They demonstrated that a combined LF-HF voltage waveform allows obtaining significant and spatially uniform deposition of the NC coating across the whole discharge area.

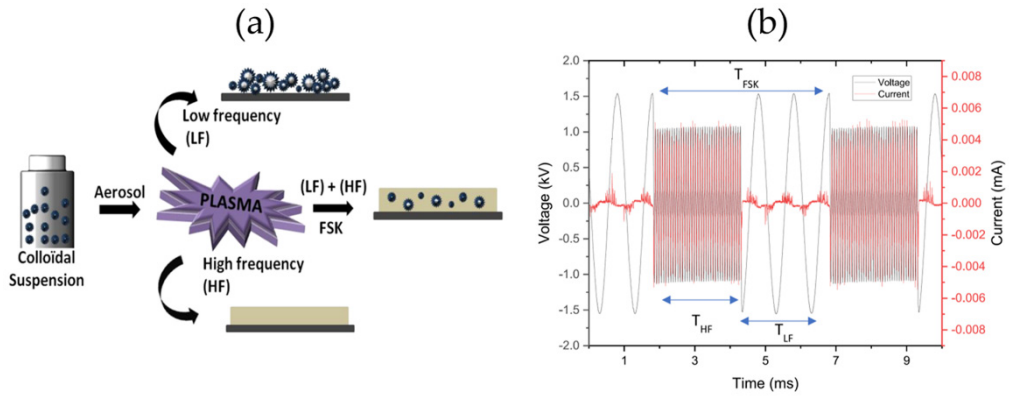

Figure 6. (**a**) Schematic representation summarizing the influence of the frequency of the sinusoidal voltage applied to the electrodes of a parallel-plate DBD system during the deposition of NC coatings from a dispersion of preformed NPs in a liquid precursor: low-frequency (LF) excitation voltage, high-frequency (HF) excitation voltage, and frequency-shift keying (FSK) modulation alternating a high-frequency and a low-frequency voltage. Reproduced with permission from [128]. (**b**) Example of a frequency-shift keying (FSK) double modulation oscillogram with frequencies of 1 kHz (LF) and 15 kHz (HF), a 50% duty cycle, and T_{FSK} of 5 ms. The high-frequency voltage is applied for 2.5 ms (T_{HF}), and the low-frequency voltage is applied for 2.5 ms (T_{LF}). Reproduced with permission from [129].

A more limited number of studies has addressed the remote AAPD of NC coatings. The first of these studies was published in 2011 by Dembele et al. [57]. This group reported the deposition of organosilicon polymer/TiO_2 NPs coatings obtained by nebulizing a dispersion of TiO_2 NPs in tetramethylorthosilicate (TMOS) into a corona-based plasma jet (Figure 2c). Different alcohols (i.e., methanol, pentanol, and octanol) were added to the dispersions to improve their stability as well as to enhance the homogeneity and growth rate of the NC coating. It was observed that, when methanol was added, the coatings were very similar to the ones deposited without alcohol addition. In contrast, octanol or pentanol addition led to coatings with greater thickness and improved homogeneity. This evidence, in conjunction with results from the chemical characterization, indicated the incorporation of octanol and pentanol in the NC coatings. The differences observed with the various alcohols were ascribed to their different boiling points (65, 136, 196 °C for of methanol, pentanol, and octanol, respectively) compared to the plasma temperature measured at the jet outlet (77 °C). Since methanol has a boiling point lower than the plasma temperature, it is expected to evaporate during the coating deposition and not to be incorporated in the coatings.

Arefi and coworkers [83] deposited photocatalytic Ag/TiO_2 NC coating with controlled porosity and crystal size by using an arc-based plasma jet. During the deposition, a dispersion of Ag NPs in titanium tetraisopropoxide was sprayed into the vicinity of the outlet of the plasma jet fed with air (Figure 7a), while the substrate temperature was

kept constant at 200 °C. After deposition, all coatings were annealed at 450°C in ambient air for 1 h. The influence of the Ag NPs concentration in the dispersion (0–0.7 wt%) and deposition parameters, such as discharge pulse frequency (18–25 kHz) and air flow rate (30–50 L·min^{-1}), were investigated on the coating structure, crystallinity, and crystal size. Through XRD investigations, it was possible to assess that the deposited Ag/TiO_2 coatings were crystalline with an anatase TiO_2 structure regardless of the pulse frequency, while the anatase crystal size depended on the experimental conditions. For instance, with increasing Ag NPs concentration in the starting dispersion, the anatase crystal size decreased, likely due to the growth inhibition induced by Ag NPs (Figure 7b). Moreover, the anatase grain size decreased with the pulse frequency, likely due to the higher energy input into the plasma (Figure 7c).

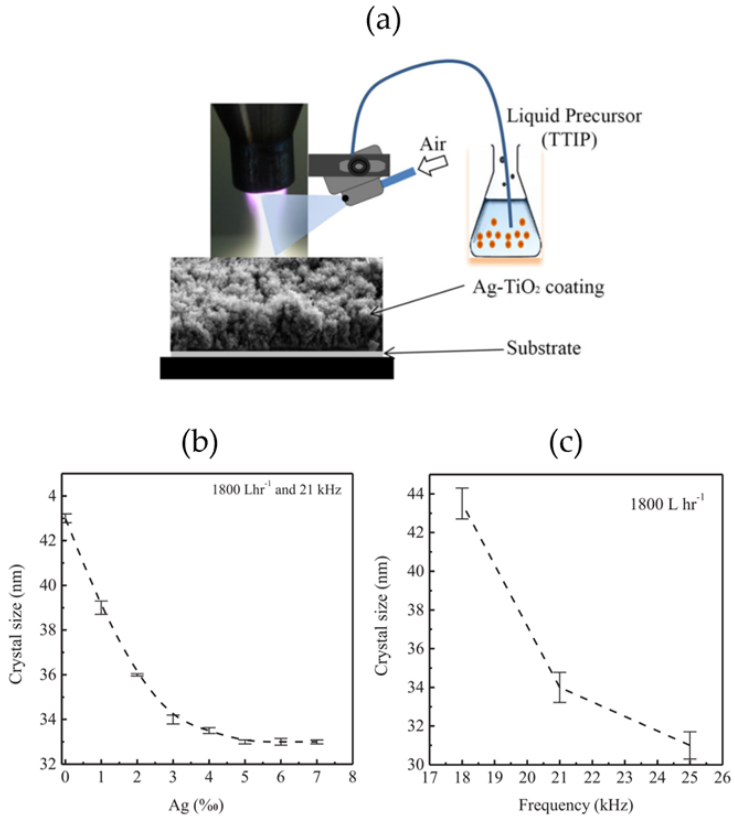

Figure 7. (**a**) Schematic of the apparatus used to deposit Ag/TiO_2 nanocomposite coating by spraying a dispersion of Ag nanoparticles in titanium tetraisopropoxide liquid precursor in the vicinity of AP plasma jet (see Figure 2d). Anatase TiO_2 crystal size in the NC coating as a function of (**b**) the Ag NPs concentration in the starting dispersion and (**c**) the discharge pulse frequency. Reproduced with permission from [83].

A different deposition approach is shown in [63,98], where the APP jet deposition of the NC thin films is accomplished by separate and simultaneous injection of the aerosol of a dispersion of inorganic NPs and the vapor of a conventional precursor. For example, Liguori et al. [63] deposited antibacterial NC coatings consisting of silver NPs embedded in a plasma-polymerized acrylic acid matrix by using a single-electrode plasma jet driven by a micropulsed generator. During the deposition processes, the aerosol of a dispersion of Ag NPs in ethanol and the vapor of acrylic acid were injected in the plasma region through two distinct channels of the plasma source. Interestingly, this deposition process allowed reaching a coating deposition rate as high as about 10 µm·min^{-1}.

4.3.2. Aerosols of Dry Particles

In this section, we present the few but important feasibility studies that appeared in the literature on the AP plasma deposition of NC coatings from dry particle aerosols (i.e., gas-borne inorganic or polymeric NPs) in conjunction with conventional molecular precursors [61,91,99,134–137]. The first study that used this approach was published in 2014 by Deng et al. [61,134]. This group deposited silver/organosilicon nanocomposite films using a corona plasma jet fed with nitrogen in mixture with oxygen, the vapor of an organosilicon precursor (tetramethyldisiloxane, TMDSO), and aerosolized Ag NPs (i.e., dry Ag NPs transported by nitrogen). The NPs aerosol was generated by injecting a nitrogen flow into a NPs feeding module, which consisted of a narrow tube filled with the NPs. It is worth noting that the authors tried also to inject in the plasma the aerosol of Ag NPs dispersions in three different solvents (H_2O, ethanol, and TMDSO); however, this led to plasma destabilization and to a very low concentration of Ag NPs in the films.

Interestingly, the works by Alexandrov et al. [91] and Tyurikov et al. [135] demonstrated the feasibility of a two-stage process for the deposition of NC coatings consisting of a molybdenum disulfide (MoS_2) nanoparticles embedded in a silicon dioxide matrix (Figure 8).

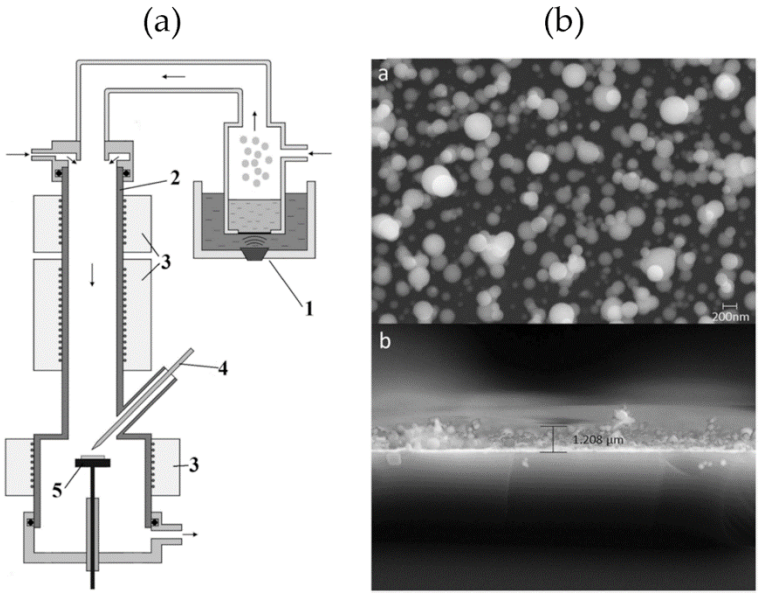

Figure 8. (**a**) Schematic diagram of the two-zone vertical reactor used in [91,135] for the AP deposition of inorganicNC coatings consisting of MoS_2 NPs embedded in a SiO_2 matrix (1, piezoelectric nebulizer; 2, quartz reactor; 3, heaters; 4, high-voltage corona electrode; 5, substrate plate). The MoS_2 NPs are synthesized in the upper zone by spray-pyrolysis, while the lower zone is used for co-depositing on the substrate surface the MoS_2 NPs and a SiO_2 layer formed by using a corona discharge fed with helium and TEOS. (**b**) Top-view and cross-sectional SEM images of the NC coatings. Reproduced with permission from [91].

Specifically, in this process, the deposition of the NC layer was performed in a vertical tubular quartz reactor consisting of two zones (Figure 8a): the upper zone was employed for the synthesis of MoS_2 NPs via spray-pyrolysis of a solution of ammonium thiomolybdate ($(NH_4)_2MoS_4$) in dimethylformamide; the lower zone was used for the co-deposition on the substrate surface of the MoS_2 particles transported by He stream from the upper zone of the reactor and a SiO_2 layer formed in a corona discharge fed with helium and TEOS. SEM observations showed that the deposited layers contain spherical particles randomly distributed in the matrix (Figure 8b) and that the average size of NPs in the layers depends on the concentration of $(NH_4)_2MoS_4$ in the starting solution. The potential of this two-stage process mainly resides in the possibility of varying the composition of the deposited

films over a wide range through independent control of the NPs synthesis and of the NC coating deposition.

Studies have been also published on the preparation of organic/inorganic NC coatings by simultaneously injecting in the AP plasma the precursor of the inorganic component of the NC (vapor or aerosol) and aerosolized polymer particles [99,136]. For example, Zuber et al. [99] successfully deposited transparent and robust nanocomposite films of polytetrafluoroethylene (PTFE) particles dispersed in a continuous SiO_x matrix by using an AP microwave plasma jet [101] fed with argon, oxygen, gas-borne PTFE micropowders, and vapors of 1,1,3,3-tetramethyldisiloxane. It was demonstrated that by changing the amount of PTFE powder injected in the plasma, it is possible to tune the polymer-to-matrix ratio of the layer as well as its properties: at low PTFE loading, the coatings are robust, transparent, and hydrophobic; and by increasing the PTFE loading, superhydrophobic coatings are obtained. Such nanocomposite films were easily deposited to a range of solid and liquid substrates (e.g., glass slides, polymer substrates, cotton cloths, droplets of liquid paraffin oil).

4.4. Deposition of NC Coatings from Aerosols of Precursor Solutions

In this section, we review the studies that combined the aerosol of a precursor solution with a low-temperature AP plasma to deposit NC thin films. This strategy represents a unique tool to use as thin film precursors inorganic salts [138–140] and a range of organic compounds, such as, for instance, proteins [141–146], drugs [65,138,147–149], diagnostic tracers [150], metalloporphyrins [80], and cyclodextrins [119]. These precursors are commonly dissolved in water [138,141,142,144,148–150] or, more rarely, in aqueous buffers [145,146] or organic solvents [139,147]. When the precursor is dissolved in either pure water or aqueous buffer, the aerosol of the resulting solution is delivered to the AP plasma in conjunction with the vapor [138,142,144,148,149] or the aerosol [142,150] of the NC matrix precursor. In contrast, when an organic solvent is used, this also acts as precursor of the NC matrix [139,147]. In both cases, the NC coating is formed through incorporation of the solute into the growing plasma-polymerized matrix.

In the following, we review the studies that explored the use of solutions of inorganic metal salts (Section 4.4.1) and of organic compounds (Section 4.4.2).

4.4.1. Solutions of Inorganic Metal Salts

When solutions of inorganic metal salts are atomized and injected in the AP plasma, the plasma ionized species can induce the reduction of the metal ion (M^{n+}) to generate metal (M) NPs, while the plasma energetic species can activate the matrix precursor which thus undergoes plasma polymerization. Consequently, the synthesis of the NPs and of the matrix occurs simultaneously in the plasma. This is the approach used by Nadal et al. [139] in a very recent work. The authors deposited plasmonic gold NPs/polymer nanocomposite thin films by using a parallel plate DBD fed with argon and the aerosol of a solution of a gold salt (i.e., $HAuCl_4 \cdot 3H_2O$) in a polymerizable solvent (i.e., isopropanol, IPA). This deposition strategy was combined with FSK double modulation of the DBD (see Section 4.3.1, Figure 6b). In particular, it was observed that: (i) the high-frequency time (T_{HF}) corresponds to the synthesis of the Au NPs in the gas phase and to the deposition of the polymer matrix (as the plasma is at the highest energy and ionization level possible); and (ii) the low-frequency time (T_{LF}) is associated with the NPs transport towards the substrate surface. An important finding of this study was the demonstration that the in-situ synthesis and deposition of the NPs and the polymer matrix allow obtaining homogeneous NC layers with non-agglomerated NPs and high NPs density. The ultraviolet-visible (UV-vis) absorption spectra confirmed the formation of Au NPs (i.e., plasmonic resonance peak centered at about 540 nm), while the atomic force microscopy (AFM) phase images revealed the presence of a thin polymer shell around the nanoparticles. The metal salt concentration in the atomized solution, the FSK parameters (i.e., duty cycle and repetition rate), and sample position along the gas flow in the DBD cell were demonstrated to affect

the size of the gold NPs, their concentration, and level of plasmonic coupling. For instance, for more concentrated starting solutions, the NPs size in the deposited layer increases, the assemblies result much denser due to the largest nucleation and higher growth rate of the NPs, and the UV-vis absorption amplitude increases.

The work by Wang et al. [140] is another example on the atmospheric pressure AAPD of NC coatings from metal salt solutions. The authors reported the deposition of antibacterial Ag-containing NC films by injecting in a parallel-plate DBD the aerosols of an aqueous $AgNO_3$ solution and HMDSO through two different pneumatic atomizers. This strategy led to the formation of organic/inorganic NC coatings featuring spherical nanocapsules. These nanocapsules exhibited a core-shell structure and, specifically, contained silver in the core and the organosilicon polymer in the shell. The effect of various experimental parameters (e.g., silver nitrate concentration in the solution, discharge power, aerosol flow rate, continuous and pulsed mode operation of the DBD) was investigated on the chemical composition and morphology of the nanostructured hybrid films.

Feasibility studies of the remote AAPD of NC coatings from metal salts solutions [151–153] have been also published. For instance, Beier et al. [151] used an APP jet to deposit Ag/SiO_x films with antibacterial properties and high abrasive-wear resistance. In this process, an aqueous $AgNO_3$ solution was sprayed into the plasma fed with air and HMDSO vapors. This led to the in-situ synthesis of silver NPs, which were incorporated in the growing SiO_x matrix.

4.4.2. Solutions of Organic Compounds

Over the last few years, remarkable advances have been made in the design and optimization of APP deposition processes from aerosols of solutions of organic compounds and, in particular, of bioactive organic molecules, such as proteins and enzymes [141–146], antibiotics and other drugs [65,138,147–149]. Since bioactive organic molecules are typically dissolved in water, during the AAPD process, the aerosolized solution is injected in the AP plasma in conjunction with the organic precursor of the polymer matrix. The resulting coatings are commonly referred to as biocomposite coatings since they incorporate bioactive agents and are therefore able to trigger specific biological responses.

The first studies that reported this strategy focused on the preparation of organic coatings loaded with either biomacromolecules, such as proteins and enzymes (e.g., glucose oxidase, lipase, elastin, lysozyme [141–146]) or small model drugs (e.g., acetaminophene) [147]. These feasibility studies demonstrated that this deposition approach offers the possibility to effectively incorporate a bioactive molecule in the coating without altering its structure and functionality thanks to the mild conditions of the AP plasma and the presence of a thin protective solvent shell around the bioactive during plasma exposure. Interestingly, in recent years, it was highlighted that very often in these coatings, the bioactive molecules localize in spatially defined nanodomains and, specifically, in the core of nanocapsules, i.e., nanometric vesicular systems consisting of a bioactive molecule-loaded cavity and a surrounding polymeric layer. Favia and coworkers investigated the deposition of NC coatings by using a parallel-plate DBD with He, ethylene, and the aerosol of an aqueous solution of antibiotic vancomycin [65,149] or gentamicin [148]. The deposited coatings consisted of antibiotic-containing spherical structures with a size of hundreds of nanometers (Figure 9). In particular, the spherical structures were nanocapsules with an antibiotic-loaded core and a hydrocarbon polymeric shell originated from the plasma polymerization of ethylene. In-depth observations with confocal fluorescence microscopy of a NC layer deposited from an aerosolized fluorescein solution (instead of the antibiotic solution) allowed better appreciating the NC structure [65]. Interestingly, fluorescence images revealed that fluorescence mainly originates from the nanocapsules due to the presence of fluorescein in the core. The authors hypothesized that this unique core-shell structure could form from the combination of aerosol droplets shrinking due to water evaporation and ethylene polymerization around the surface of the aerosol droplets. Due to this unique morphology, the deposited coatings demonstrated to be suitable for drug delivery applications (see Section 5.4). We re-

fer readers interested in the formation of nanocapsules as well as in the experimental parameters that influence their shape, size, and number density to a number of recent papers [70,138,148,149]. For example, Palumbo et al. [148] investigated the effect of the electrical conditions used to generate the DBD (i.e., continuous and pulsed mode, high and low input power) on the morphology of gentamicin-loaded NC coatings and, in particular, on the dimension and distribution of the nanocapsules. SEM observations revealed that: (a) under continuous plasma conditions and at high input power, the gentamycin-loaded coatings exhibit a more uniform size distribution of spherical features (Figure 9a); (b) under pulsed plasma conditions and at high power, a broader size distribution of slightly smaller nanocapsules is observed (Figure 9b); and (c) under continuous plasma conditions and at low power, the nanocapsules present a similar average diameter but decreased surface density compared with those formed in continuous mode and at higher power (Figure 9c).

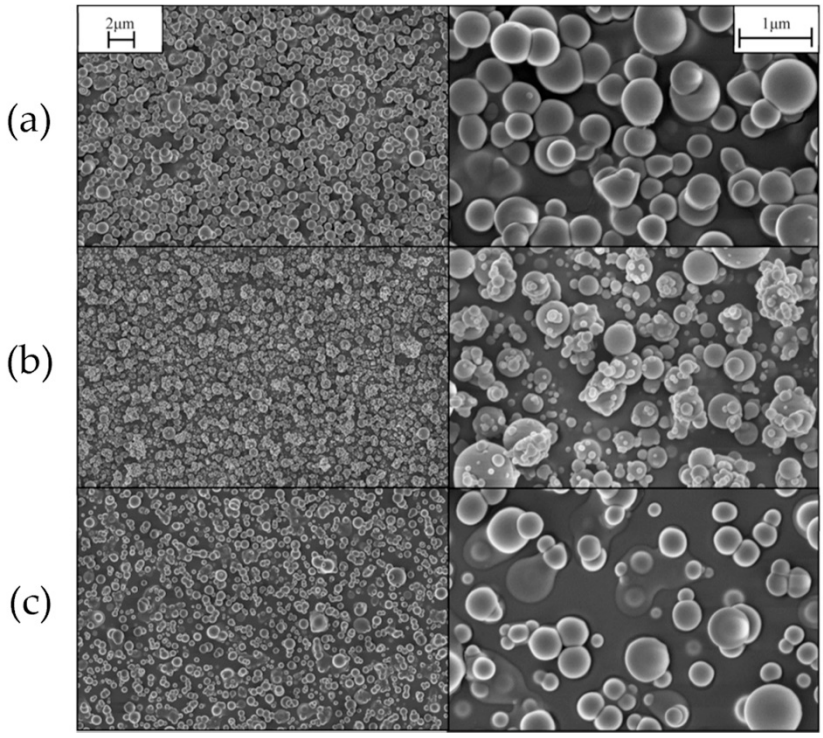

Figure 9. SEM images (at a magnification of 10k×, left and 50k×, right) of gentamicin-loaded NC coatings deposited for 20 min in a parallel-plate DBD fed with helium, ethylene, and an aqueous gentamicin solution (10 mg/mL). The DBD is generated using different electrical excitation conditions: (**a**) continuous mode, high power; (**b**) pulsed mode, high power; (**c**) continuous mode, low power. Reproduced with permission from [148].

5. Functional Properties of NC Coatings Deposited by APPs

In this section, we provide an overview of the most common functional properties of APP-deposited NC coatings. On the basis of the available literature, we also identify various potential applications and define areas where further research is needed.

5.1. Catalytic Properties

Considerable research efforts have been devoted to the design and development of photocatalytic NC coatings for wastewater treatment [32,83,125,126] and self-cleaning applications [66,84] (Table 1). In particular, a number of recent studies focused on the APP deposition of TiO_2- or ZnO-containing NC coatings and on the optimization of their photocatalytic activity towards the degradation of organic pollutants in water. These photocatalytic NC coatings include: (i) inorganic coatings (e.g., Ag/TiO_2 or TiO_2/SiO_2) obtained by either PECVD or AAPD processes [66,83,84]; and (ii) hybrid organic/inorganic coatings

(e.g., hydrocarbon polymer/ZnO NPs or hydrocarbon polymer/TiO_2 NPs) prepared by AAPD from dispersions of preformed metal oxide NPs in the liquid precursor of the organic matrix [60,125,126]. It has been highlighted that the highly porous structure [66,83,125] of APP-deposited NC coatings is particularly important for catalytic applications and, for instance, leads to increased photocatalytic activity. Interestingly, Peng et al. [83] demonstrated that enhanced visible-light photocatalytic activity can be achieved through incorporation of Ag nanoparticles in porous anatase TiO_2 coatings by using a facile, remote AAPD strategy. In addition, a very recent work [125] confirmed the potential of low temperature AP plasmas for the well-controlled deposition of TiO_2-based NC coatings on complex geometry substrates, such as open-cell polyurethane foams. This study revealed that enhanced photocatalytic activity can be achieved by using these substrates due to their 3D macroporous structure, which ensures large interface for reaction and superior light-harnessing capabilities ([125] and references therein).

Table 1. Representative studies on photocatalytic NC coatings deposited by APPs.

Coating Composition	Plasma Source/ Deposition Process	Precursors	Application	Reference
Ag/TiO_2	Arc jet/ Remote AAPD	Dispersion of Ag NPs in TTIP	Dyes and drugs degradation in water	[83]
TiO_2/SiO_2	Arc jet/ Remote AAPD	TTIP + HMDSO	Self-cleaning surfaces	[66]
TiO_x/SiO_x	Arc jet/ Remote PECVD	TEOS + TTIP	Self-cleaning and antimicrobial surfaces	[84]
ZnO/hydrocarbon polymer	DBD/ Direct AAPD	Dispersion of oleate-capped ZnO NPs in n-octane/1,7-octadiene	Dye degradation in water	[32,126]
TiO_2/hydrocarbon polymer	DBD/ Direct AAPD	Dispersion of oleate-capped TiO_2 NPs in n-octane/1,7-octadiene	Dye degradation in water	[125]

TTIP, titanium tertraisopropoxide; TEOS, tetraethyl orthosilicate; HMDSO, hexamethydisiloxane.

To the best of our knowledge, the work by Michel et al. [55] remains the only paper that has focused on another class of catalytic NC coatings. The authors investigated the atmospheric pressure AAPD of plasma-polymerized polyaniline films embedding Pt nanoparticles. In particular, these films consisted of a dense three-dimensional porous network of PANI-Pt fibers (diameter in the range 50–70 nm) and exhibited promising catalytic properties for fuel cell applications.

To close this section, it is also important to mention the studies reporting the atmospheric pressure AAPD of biocomposite coatings loaded with enzymes [144,146], i.e., biocatalysts able to accelerate many biochemical and chemical reactions. These studies pave the way to novel APPs-based strategies for the facile and efficient enzyme immobilization onto solid supports [154] for potential application in diverse fields (e.g., industrial biocatalysis, biosensing, various biotechnological applications).

5.2. Corrosion Resistance Properties

The plasma deposition of corrosion-protective coatings on metal substrates received enormous attention in the last decades and still continues nowadays to attract considerable interest [155,156]. In particular, organosilicon and SiO_2-like coatings deposited by low pressure PECVD have been widely and successfully used for the corrosion protection of various metals (e.g., steel, magnesium alloys, silver) [155,157]. In contrast, a very limited number of studies assessed the applicability of analogous coatings deposited in AP plasmas (see, for example, [158,159]). However, it has been recently reported that the incorporation of small amounts of inorganic nanoobjects in an AP plasma-deposited

organosilicon polymer can lead to improved anticorrosion properties [54,67]. For example, Anagri et al. [67] successfully developed anticorrosion NC coatings by atomizing into a DBD reactor a dispersion of graphene nanosheets (GNs) in a liquid organosilicon precursor (i.e., HMDSO). Steel substrates coated with the hybrid GNs/organosilicon polymer layers exhibited significantly improved resistance to corrosive media as compared to those coated with the organosilicon layer alone. This is likely due to the additional physical barrier offered by graphene nanosheets. The authors also showed that the pretreatment of the steel substrates with an air-fed APP jet (see Figure 2d) immediately prior to coating deposition enhances the coating-substrate performances. The beneficial effect of the pretreatment was ascribed to various factors, including the removal of surface contaminants (e.g., hydrocarbon layer), the formation of a passivation layer, and the improvement of the coating-metal adhesion [67,155].

Bardon et al. [54] reported on the direct AAPD deposition of hybrid NC coatings consisting of $AlCeO_3$ NPs embedded in an organosilicon polymer. Due to the presence of the $AlCeO_3$ NPs, these NC coatings exhibited self-healing properties and hence increased corrosion protection performances.

5.3. Optical Properties

Various studies explored the possibility to use low-temperature AP plasmas for the preparation of nanocomposite films with tailored optical properties (Table 2). For example, the deposition of luminescent or photoluminescent NC films was investigated in [59] and [98], respectively. Boscher et al. [59] prepared luminescent, lanthanide-based hybrid coatings by using an aerosol-assisted strategy. In the deposition process, a dispersion composed of optically active lanthanide-containing coordination polymer particles, hexamethyldisiloxane (HMDSO), and ethanol was sprayed onto the surface of aluminum or polypropylene foils prior to AP plasma exposure.

Table 2. Representative studies on APP-deposited NC coatings with specific optical properties.

Coating Composition	Plasma Source/ Deposition Process	Precursors	Application	Reference
Lantanide-containing coordination polymer/SiOx	DBD/ Direct AAPD	Dispersion of lantanide-containing coordination polymer NPs in HMDSO/ethanol	Luminescence-based applications	[59]
ZnO/hydrocarbon polymer	Arc jet/ Remote AAPD	Dispersion of ZnO NPs in water (aerosol) + hexane (vapor)	Photoluminescence-based applications	[98]
Zn(TPP)/organosilicon polymer	DBD/ Direct AAPD	Solution of Zn(TPP) in HMDSO and ethanol or chloroform (aerosol) + HMDSO (vapor)	Colorimetric gas sensors	[80]
TiO_2/polyester	Arc jet/ Remote AAPD	Polyester powder (aerosol) + TTIP (aerosol)	UV protection	[136]
Au/ppIPA	DBD/ Direct AAPD	Solution of gold salt ($HAuCl_4 \cdot 3H_2O$) in IPA	Plasmonics	[139]

HMDSO, hexamethydisiloxane; Zn(TPP), zinc 5,10,15,20-tetraphenylporphyrin; TTIP, titanium tetraisopropoxide; ppIPA, plasma-polymerized isopropyl alcohol; IPA, isopropyl alcohol (isopropanol).

UV-protective NC thin films coatings were also fabricated by Jnido et al. [136]. These authors deposited on wood samples a TiO_2/polyester film by using an AP arc jet fed with air, titanium tetraisopropoxide, and polyester powders. The coated-samples were demonstrated to undergo a minor discoloration when exposed to UV irradiation as compared to the uncoated samples [136].

Interestingly, very recently, Nadal et al. [139] demonstrated that it is possible to obtain plasmonic layers characterized by uniform insertion of Au NPs into a polymer matrix by injecting in the AP plasma the aerosol of a gold salt solution in isopropanol. Interestingly, the authors showed that the plasmonic optical response of the hybrid layers depends on the NPs size, morphology, and spatial arrangement, which in turn can be controlled by varying the deposition conditions. These coatings could find potential applications in various fields (e.g., medical imaging, biotechnology, photovoltaics).

In spite of the recent progress made, it is important to note that significant research efforts are still needed to achieve the outstanding optical performances of NC coatings deposited by LP plasmas [160–162]. LP plasma deposition processes allow achieving very precise control of the chemical composition, structure, and morphology of the NC coatings and thus enable fine-tuning of various properties, such as optical transparency, refractive index, and plasmonic response.

5.4. Antibacterial Properties

Over the last decade, APP plasmas have been widely used for the deposition of antibacterial NC coatings (Table 3). These can be divided into two classes: metal NPs-containing coatings and drug-loaded coatings.

Table 3. Representative studies on antibacterial NC coatings deposited by APPs.

Coating Composition	Plasma Source/ Deposition Process	Precursors	Property	Reference
Ag/organosilicon polymer	DBD/ Direct AAPD	Solution of $AgNO_3$ in water + HMDSO	Antibacterial property based on Ag^+ release	[140]
Ag/organosilcon polymer	Arc jet/ Remote AAPD	Ag NPs powder (aerosol) + TDMSO (vapor)	Antibacterial property based on Ag^+ release	[61]
Ag/ppAA	Arc jet/ Remote AAPD	Dispersion of Ag NPs in ethanol (aerosol) + AA (vapor)	Antibacterial property based on Ag^+ release	[63]
Ag/SiO_x	Arc jet/ Remote AAPD	Solution of $AgNO_3$ in water/IPA (aerosol) + HMDSO (vapor)	Antibacterial property based on Ag^+ release	[151,152]
Zn/SiO_x Cu/SiO_x	Arc jet/ Remote AAPD	Solution of $Zn(NO_3)_2$ or $Cu(NO_3)_2$ in water/IPA (aerosol) + HMDSO (vapor)	Antibacterial property based on Zn^{2+} or Cu^{2+} release	[153]
Vancomycin/hydrocarbon polymer	DBD/ Direct AAPD	Solution of vancomycin hydrochloride in water (aerosol) + ethylene	Antibacterial property based on drug release	[149]
Gentamicin/hydrocarbon polymer	DBD/ Direct AAPD	Solution of gentamicin sulfate in water (aerosol) + ethylene	Antibacterial property based on drug release	[148]

HMDSO, hexamethydisiloxane; TDMSO, 1,1,3,3-tetramethyldisiloxane; ppAA, plasma-polymerized acrylic acid; AA, acrylic acid.

The first class of antibacterial coatings is generally prepared by AAPD from an Ag NPs dispersion [63] or a metal salt solution (e.g., aqueous solution of $AgNO_3$ [140,151,152], $Zn(NO_3)_2$ [153], or $Cu(NO_3)_2$ [153]). The antibacterial activity of these coatings is attributed to the controlled release of metal ions (e.g., Ag^+, Zn^{2+}, Cu^{2+}) when in contact with water [63,140,151–153].

The preparation of the second class of antibacterial coating relies on the injection in the APPs of an aqueous drug solution (e.g., vancomycin or gentamicin antibiotics [65,138,148,149]) and a plasma-polymerizable organic precursor. As previously described (Section 4.4), this deposition strategy leads to the preparation of hybrid coatings containing drug-loaded nanocapsules. In particular, in [65,138,149], it was shown that, upon water immersion,

the nanocapsules become empty or collapse, leading to effective drug release in the aqueous medium. Overall, these coatings have great potential for addressing various challenges in the field of drug delivery.

5.5. Wettability Properties

It has been widely reported that organic/inorganic NC thin films consisting of polymers and inorganic NPs can exhibit superhydrophobic behavior, i.e., water contact angle (WCA) > 150° and contact angle hysteresis < 10° [162–165]. This behavior is due to the combination of a low surface energy organic component and an adequate surface roughness induced by NPs incorporation. Various studies demonstrated that the atmospheric pressure AAPD from dispersions of inorganic NPs in an organic solvent enables the fast and facile deposition of superhydrophobic NC coatings [32,60,124,126,128] (Table 4). In particular, the studies by Fanelli et al. [60,126] revealed that the spatial organization of the organic and inorganic components in these NC coatings is particularly suitable for obtaining low hysteresis superhydrophobic properties: i.e., the low surface energy polymer dominates the surface chemical composition of the NC coating, while NPs form quasi-spherical agglomerates inducing a hierarchical multiscale surface texture (Figures 4a and 5). The wetting properties of the NC coatings can be tuned by simply varying the composition of the starting dispersion (e.g., NPs concentration, volume fraction of an additive) [60,124] or the electrical conditions used for plasma generation (e.g., FSK modulation parameters [128], see Section 4.3). It is worth mentioning that the presence of NPs agglomerates in the coatings, while beneficial to obtain superhydrophobic properties, can severely compromise the durability and the optical transparency of the coatings. Therefore, current research efforts are focused on obtaining robust and transparent superhydrophobic NC coatings by APPs [60,99,124,136]. Broadly, the interest toward thin films with superhydrophobic properties concerns their ability to repel water and be self-cleaning and/or anti-stick. However, it is very important to consider that when dealing with organic/inorganic NC coatings efforts are very often directed to obtain multifunctional coatings. In fact, the proper selection of the embedded NPs allows developing multifunctional coatings that, in addition to superhydrophobic properties, simultaneously offer other functionalities, such as catalytic activity, anticorrosion resistance, and antibacterial properties [126,165].

Table 4. Representative studies on APP-deposited NC coatings with superhydrophobic or special wettability properties.

Coating Composition	Plasma Source/ Deposition Process	Precursors	Wettability Behavior	Reference
ZnO/hydrocarbon polymer	DBD/ Direct AAPD	Dispersion of oleate-capped ZnO NPs in n-octane/1,7-octadiene	Superhydrophobicity	[32,60,124,126]
TiO_2/ppIPA	DBD/ Direct AAPD	Dispersion of TiO_2 NPs in IPA	Superhydrophobicity	[128]
TiO_2/ppIPA	DBD/ Direct AAPD	Dispersion of TiO_2 NPs in IPA	Superhydrophobicity	[133]
PTFE/SiO_x	Arc jet/ Remote AAPD	PTFE powder (aerosol) + TDMSO (vapor)	Superhydrophobicity	[99]
TiO_2/polyester	Arc jet/ Remote AAPD	Polyester powder (aerosol) + TTIP (aerosol)	Superhydrophobicity	[136]
POSS/organosilicon polymer	DBD/ Direct AAPD	Dispersion of POSS NPs in HMDSO	Contemporaneous hydrophobicity/ alcoholphilicity	[132]

ppIPA, plasma-polymerized isopropyl alcohol; IPA, isopropyl alcohol (isopropanol); PTFE, polytetrafluoroethylene; TDMSO, 1,1,3,3-petramethyldisiloxane; TTIP, titanium tetraisopropoxide; POSS, polyhedral oligomeric silsesquioxane; HMDSO, hexamethydisiloxane.

Finally, it is worth mentioning the work by Chen et al. [132] that reported on the preparation of hybrid coatings with selective wettability with respect to different solvents

(water and organic solvents). In particular, in this study, an AAPD process was used to deposit NC coatings consisting of octamethyl-polyhedral oligomeric silsesquioxane (octametyl-POSS) powders embedded in an organosilicon polymer. These coatings exhibited contemporaneous hydrophobic and alcohol-philic properties, offering separation factors of ethanol over water up to 6.5.

6. Conclusions

Low-temperature AP plasma technology is in a stage of great vitality in a range of application fields. The present paper provides a critical review of APP processes recently designed and optimized for the deposition of nanocomposite coatings. We have highlighted that, while the NC coatings prepared by using AP plasmas cannot offer the same properties of those deposited in LP plasmas, APP processes have distinctive features and advantages that have opened unprecedented opportunities for the fabrication of novel multicomponent materials in thin film form.

APP reactors have been developed in a wide range of configurations, allowing the design of a variety of PECVD and AAPD methods and therefore the synthesis of very diverse coatings, in terms of chemical, morphological, and functional properties. An increasing important role is played by aerosol-assisted plasma processes, which enable the use of unconventional precursors, such as dispersions and solutions. Interestingly, considerable progress has been made in the understanding of the fundamental mechanisms and key parameters that control the growth of the NC layers in the AP plasma.

As far as the functional properties and possible applications of the deposited coatings are concerned, some important research trends have emerged in recent years. They currently include the preparation of organic/inorganic NC coatings with superhydrophobic properties or opposite wettability behavior towards different liquids; the fabrication of drug-loaded coatings with potential application as drug delivery system; the synthesis of highly-porous photocatalytic NC coatings for wastewater treatment; as well as the effective incorporation of either catalytic inorganic NPs or biocatalysts (i.e., enzymes) in hybrid layers deposited on different substrates (including open-cell polymer foams).

Current challenges mainly lie in reducing the NPs agglomeration in the coatings as well as in improving the quality of the deposited layers, for example, in terms of chemical and mechanical durability, and of optical properties. Future efforts should be directed to evaluate the feasibility of using the most promising deposition methods for large-scale applications.

Author Contributions: Conceptualization, F.F.; bibliographic search, A.U.; writing—original draft preparation, A.U. and F.F.; writing—review and editing, F.F.; supervision, F.F.; funding acquisition, F.F. All authors have read and agreed to the published version of the manuscript.

Funding: This research was funded by the Italian Ministry for University and Research (MUR) under grant ARS01_00849. A.U. gratefully acknowledges Italian Ministry for Education, University, and Research (MIUR) for funding her PhD research fellowship (PON FSE-FESR Research and Innovation 2014–2020).

Institutional Review Board Statement: Not applicable.

Informed Consent Statement: Not applicable.

Conflicts of Interest: The authors declare no conflict of interest.

References

1. Mariotti, D.; Sankaran, R.M. Microplasmas for nanomaterials synthesis. *J. Phys. D Appl. Phys.* **2010**, *43*, 323001. [CrossRef]
2. Massines, F.; Sarra-Burnet, C.; Fanelli, F.; Naudé, N.; Gherardi, N. Atmospheric pressure low temperature direct plasma technology: Status and challenges for thin film deposition. *Plasma Process. Polym.* **2012**, *9*, 1041–1073. [CrossRef]
3. Mariotti, D.; Belmonte, T.; Benedickt, J.; Velusamy, T.; Jain, G.; Svrcek, V. Low-temperature atmospheric pressure plasma processes for "green" third generation photovoltaics. *Plasma Process. Polym.* **2016**, *13*, 70–90. [CrossRef]

4. Fanelli, F.; Fracassi, F. Atmospheric pressure non-equilibrium plasma jet technology: Atmospheric pressure non-equilibrium plasma jet technology: General features, specificities and applications in surface processing of materials. *Surf. Coat. Technol.* **2017**, *322*, 174–201. [CrossRef]
5. Dimitrakellis, P.; Gogolides, E. Hydrophobic and superhydrophobic surfaces fabricated using atmospheric pressure cold plasma technology: A review. *Adv. Colloid Interface Sci.* **2018**, *254*, 1–21. [CrossRef]
6. Cvelbar, U.; Walsh, J.L.; Cernak, M.; de Vries, H.W.; Reuter, S.; Belmonte, T.; Corbella, C.; Miron, C.; Hojnik, N.; Jurov, A.; et al. White paper on the future of plasma science and technology in plastics and textiles. *Plasma Process. Polym.* **2019**, *16*, e1700228. [CrossRef]
7. Chiang, W.; Mariotti, D.; Sankaran, R.M.; Erden, J.G.; Ostrikov, K. Microplasmas for advanced materials and devices. *Adv. Mater.* **2020**, *32*, 1905508. [CrossRef]
8. Wang, L.; Yi, Y.; Guo, H.; Tu, X. Atmospheric pressure and room temperature synthesis of methanol through plasma-catalytic hydrogenation of CO_2. *ACS Catal.* **2018**, *8*, 90–100. [CrossRef]
9. Li, S.; Medrano, J.A.; Hessel, V.; Gallucci, F. Recent progress of plasma-assisted nitrogen fixation research: A review. *Processes* **2018**, *6*, 248. [CrossRef]
10. Delikonstantis, E.; Scapinello, M.; Stefanidis, G.D. Process modeling and evaluation of plasma-assisted ethylene production from methane. *Processes* **2019**, *7*, 68. [CrossRef]
11. Li, J.; Ma, C.; Zhu, S.; Yu, F.; Dai, B.; Yang, D. A review of recent advances of dielectric barrier discharge plasma in catalysis. *Nanomaterials* **2019**, *9*, 1428. [CrossRef]
12. Pang, Y.; Hammer, T.; Müller, D.; Karl, J. Investigation of nonthermal plasma assisted charcoal gasification for production of hydrogen-rich syngas. *Processes* **2019**, *7*, 114. [CrossRef]
13. Taheraslani, M.; Gardeniers, H. Plasma catalytic conversion of CH_4 to alkanes, olefins and H_2 in a packed bed DBD reactor. *Processes* **2020**, *8*, 774. [CrossRef]
14. Bogaerts, A.; Tu, X.; Whitehead, J.C.; Centi, G.; Lefferts, L.; Guaitella, O.; Azzolina-Jury, F.; Kim, H.-H.; Murphy, A.B.; Schneider, W.F.; et al. The 2020 plasma catalysis roadmap. *J. Phys. D Appl. Phys.* **2020**, *53*, 443001. [CrossRef]
15. Centi, G.; Perathoner, S. Redesign chemical processes to substitute the use of fossil fuels: A viewpoint of the implications on catalysis. *Catal. Today* **2021**, in press. [CrossRef]
16. Brandenburg, R.; Bogaerts, A.; Bongers, W.; Fridman, A.; Fridman, G.; Lockers, B.R.; Miller, V.; Reuter, S.; Schiorlin, M.; Verreycken, T.; et al. White paper on the future of plasma science in environment, for gas conversion and agriculture. *Plasma Process. Polym.* **2019**, *16*, e1700238. [CrossRef]
17. Shukrullah, S.; Bashir, W.; Altaf, N.U.H.; Khan, Y.; Al-Arainy, A.A.; Sheikh, T.A. Catalytic and non-catalytic treatment of industrial wastewater under the exposure of non-thermal plasma jet. *Processes* **2020**, *8*, 667. [CrossRef]
18. Laroussi, M. Plasma medicine: A brief introduction. *Plasma* **2018**, *1*, 47–60. [CrossRef]
19. Gupta, T.T.; Ayan, H. Application of non-thermal plasma on biofilm: A review. *Appl. Sci.* **2019**, *9*, 3548. [CrossRef]
20. Semmler, M.L.; Bekeschus, S.; Schäfer, M.; Bernhardt, T.; Fischer, T.; Witzke, K.; Seebauer, C.; Rebl, H.; Grambow, E.; Vollmar, B.; et al. Molecular mechanisms of the efficacy of cold atmospheric pressure plasma (CAP) in cancer treatment. *Cancers* **2020**, *12*, 269. [CrossRef]
21. Pankaj, S.K.; Wan, Z.; Keener, K.M. Effects of cold plasma on food quality: A review. *Foods* **2018**, *7*, 4. [CrossRef]
22. Attri, P.; Ishikawa, K.; Okumura, T.; Koga, K.; Shiratani, M. Plasma agriculture from laboratory to farm: A review. *Processes* **2020**, *8*, 1002. [CrossRef]
23. Adhikari, B.; Adhikari, M.; Park, G. The effects of plasma on plant growth, development, and sustainability. *Appl. Sci.* **2020**, *10*, 6045. [CrossRef]
24. Fridman, A.; Chirokov, A.; Gutsol, A. Non-thermal atmospheric pressure discharges. *J. Phys. D Appl. Phys.* **2005**, *38*, R1–R24. [CrossRef]
25. Laimer, J.; Störi, H. Recent advances in the research on non-equilibrium atmospheric pressure plasma jets. *Plasma Process. Polym.* **2007**, *4*, 266–274. [CrossRef]
26. Iza, F.; Kim, G.J.; Lee, S.M.; Lee, J.K.; Walsh, J.L.; Zhang, Y.T.; Kong, M.G. Microplasmas: Sources, particle kinetics, and biomedical applications. *Plasma Process. Polym.* **2008**, *5*, 322–344. [CrossRef]
27. Bardos, L.; Barankova, H. Cold atmospheric plasma: Sources, processes, and applications. *Thin Solid Films* **2010**, *518*, 6705–6713. [CrossRef]
28. Brandenburg, R. Dielectric barrier discharges: Progress on plasma sources and on the understanding of regimes and single filaments. *Plasma Sources Sci. Technol.* **2017**, *26*, 053001. [CrossRef]
29. Bruggeman, P.J.; Iza, F.; Brandenburg, R. Foundations of atmospheric pressure non-equilibrium plasmas. *Plasma Sources Sci. Technol.* **2017**, *26*, 123002. [CrossRef]
30. Belmonte, T.; Henrion, G.; Gries, T. Nonequilibrium atmospheric plasma deposition. *J. Therm. Spray Technol.* **2011**, *20*, 744–759. [CrossRef]
31. Jang, H.J.; Jung, E.Y.; Parsons, T.; Tae, H.-S.; Park, C.-S. A review of plasma synthesis methods for polymer films and nanoparticles under atmospheric pressure conditions. *Polymers* **2021**, *13*, 2267. [CrossRef]
32. Fanelli, F.; Bosso, P.; Mastrangelo, A.M.; Fracassi, F. Thin film deposition at atmospheric pressure using dielectric barrier discharges: Advances on three-dimensional porous substrates and functional coatings. *Jpn. J. Appl. Phys.* **2016**, *55*, 07LA01. [CrossRef]
33. Bosso, P.; Fanelli, F.; Fracassi, F. Deposition of water-stable coatings containing carboxylic acid groups by atmospheric pressure cold plasma jet. *Plasma Process. Polym.* **2016**, *13*, 217–226. [CrossRef]
34. Banerjee, S.; Adhikari, E.; Sapkota, P.; Sebastian, A.; Ptasinska, S. Atmospheric pressure plasma deposition of TiO_2: A review. *Materials* **2020**, *13*, 2931. [CrossRef]

35. Fanelli, F.; Di Renzo, G.; Fracassi, F.; d'Agostino, R. Recent advances in the atmospheric pressure PE-CVD of fluorocarbon films: Influence of air and water vapour impurities. *Plasma Process. Polym.* **2009**, *6*, S503–S507. [CrossRef]
36. Meshkova, A.S.; Elam, F.M.; Starostin, S.A.; van de Sanden, M.C.M.; de Vries, H.W. The role of carrier gas flow in roll-to-roll AP-PECVD synthesized silica moisture barrier films. *Surf. Coat. Technol.* **2018**, *339*, 20–26. [CrossRef]
37. Barillas, L.; Makhneva, E.; Weltmann, K.-D.; Seitz, H.; Fricke, K. Plasma printing-direct local patterning with functional polymer coating for biosensing and microfluidics applications. *Microelectron. Eng.* **2020**, *233*, 111431. [CrossRef]
38. Zhao, O.; Ding, Y.; Pan, Z.; Rolston, N.; Zhang, J.; Dauskardt, R.H. Open-air plasma-deposited multilayer thin-film moisture barriers. *ACS Appl. Mater. Interfaces* **2020**, *12*, 26405–26412. [CrossRef]
39. Acharya, K.; Bulou, S.; Gaulain, T.; Gerard, M.; Choquet, P. Site-selective atmospheric pressure plasma-enhanced chemical vapor deposition process for micrometric deposition of plasma-polymerized methyl methacrylate. *Plasma Process. Polym.* **2021**, *18*, e2000143. [CrossRef]
40. Eichler, M.; Nagel, K.; Hennecke, P.; Klages, C.-P. Area-selective microplasma treatment in microfluidic channels for novel fluid phase separators. *Plasma Process. Polym.* **2012**, *9*, 1160–1167. [CrossRef]
41. Pothiraja, R.; Engelhardt, M.; Bibinov, N.; Awakowicz, P. Film deposition on the inner surface of tubes using atmospheric-pressure Ar–CH_4, Ar–C_2H_2 and Ar–C_2H_2–H_2 plasmas: Interpretation of film properties from plasma-chemical kinetics. *J. Phys. D Appl. Phys.* **2012**, *45*, 335202. [CrossRef]
42. Fanelli, F.; Fracassi, F. Thin film deposition on open-cell foams by atmospheric pressure dielectric barrier discharges. *Plasma Process. Polym.* **2016**, *13*, 470–479. [CrossRef]
43. Armenise, V.; Milella, A.; Fracassi, F.; Bosso, P.; Fanelli, F. Deposition of thin films containing carboxylic acid groups on polyurethane foams by atmospheric pressure non-equilibrium plasma jet. *Surf. Coat. Technol.* **2019**, *379*, 125017. [CrossRef]
44. Michlicek, M.; Manakhov, A.; Dvorakova, E.; Zajickova, L. Homogeneity and penetration depth of atmospheric pressure plasma polymerization onto electrospun nanofibrous mats. *Appl. Surf. Sci.* **2019**, *471*, 835–841. [CrossRef]
45. Palumbo, F.; Lo Porto, C.; Fracassi, F.; Favia, P. Recent advancements in the use of aerosol-assisted atmospheric pressure plasma deposition. *Coatings* **2020**, *10*, 440. [CrossRef]
46. Cui, L.; Ranade, A.N.; Matos, M.A.; Dubios, G.; Dauskardt, R.H. Improved adhesion of dense silica coatings on polymers by atmospheric plasma pretreatment. *ACS Appl. Mater. Interfaces* **2013**, *5*, 8495–8504. [CrossRef] [PubMed]
47. Lelievre, J.-F.; Kafle, B.; Saint-Cast, P.; Brunet, P.; Magnan, R.; Hernandez, E.; Pouliquen, S.; Massines, F. Progress in efficient silicon nitride SiN_x:H antireflective and passivation layers deposited by atmospheric pressure PECVD for silicon solar cells. *Prog. Photovolt. Res. Appl.* **2019**, *27*, 1007–1019. [CrossRef]
48. Malinowski, S.; Herbert, P.A.F.; Rogalski, J.; Jaroszyńska-Wolińska, J. Laccase enzyme polymerization by soft plasma jet for durable bioactive coatings. *Polymers* **2018**, *10*, 532. [CrossRef]
49. Loyer, F.; Combrisson, A.; Omer, K.; Moreno-Couranjou, M.; Choquet, P.; Boscher, N.D. Thermoresponsive water-soluble polymer layers and water-stable copolymer layers synthesized by atmospheric plasma initiated chemical vapor deposition. *ACS Appl. Mater. Interfaces* **2019**, *11*, 1335–1343. [CrossRef]
50. Moreno-Couranjou, M.; Guillot, J.; Audinot, J.-N.; Bour, J.; Prouvé, E.; Durrieu, M.-C.; Choquet, P.; Detrembleurs, C. Atmospheric pulsed plasma copolymerization of acrylic monomers: Kinetics, chemistry, and applications. *Plasma Process. Polym.* **2020**, *17*, e1900187. [CrossRef]
51. Buxadera-Palomero, J.; Fricke, K.; Reuter, S.; Gil, F.J.; Rodriguez, D.; Canal, C. One-step liquid phase polymerization of HEMA by atmospheric-pressure plasma discharges for Ti dental implants. *Appl. Sci.* **2021**, *11*, 662. [CrossRef]
52. Work, W.J.; Horie, K.; Hess, M.; Stepto, F.T. Definition of terms related to polymer blends, composites, and multiphase polymeric materials (IUPAC Recommendations 2004). *Pure Appl. Chem.* **2004**, *11*, 1985–2007. [CrossRef]
53. Alemán, J.V.; Chadwick, A.V.; He, J.; Hess, M.; Horie, K.; Jones, R.G.; Kratochvíl, P.; Meisel, I.; Mita, I.; Moad, G.; et al. Definitions of terms relating to the structure and processing of sols, gels, networks, and inorganic-organic hybrid materials (IUPAC Recommendations 2007). *Pure Appl. Chem.* **2007**, *79*, 1801–1829. [CrossRef]
54. Bardon, J.; Bour, J.; Del Frari, D.; Arnoult, C.; Ruch, D. Dispersion of cerium-based nanoparticles in an organosilicon plasma polymerized coating: Effect on corrosion protection. *Plasma Process. Polym.* **2009**, *6*, S655–S659. [CrossRef]
55. Michel, M.; Bour, J.; Petersen, J.; Arnoult, C.; Ettingshausen, F.; Roth, C.; Ruch, D. Atmospheric plasma deposition: A new pathway in the design of conducting polymer-based anodes for hydrogen fuel cells. *Fuel Cells* **2010**, *6*, 932–937. [CrossRef]
56. Dowling, D.P.; Twomey, B.; Byrne, G. Effect of titanium oxide nanoparticle incorporation into nm thick coatings deposited using an atmospheric pressure plasma. *J. Nanosci. Nanotechnol.* **2010**, *10*, 2746–2752. [CrossRef]
57. Dembele, A.; Rahman, M.; Reid, I.; Twomey, B.; MacElroy, J.M.D.; Dowling, D.P. Deposition of hybrid organic-inorganic composite using an atmospheric plasma jet system. *J. Nanosci. Nanotechnol.* **2011**, *11*, 8730–8737. [CrossRef]
58. Uygun, A.; Oksuz, L.; Yavuz, A.G.; Gulec, A.; Sen, S. Characterization of nanocomposite films deposited by atmospheric pressure uniform RF glow plasma. *Curr. Appl. Phys.* **2011**, *11*, 250–254. [CrossRef]
59. Boscher, N.D.; Choquet, P.; Duday, D.; Kerbellec, N.; Lambrechts, J.-C.; Maurau, R. Luminescent lanthanide-based hybrid coatings deposited by atmospheric pressure plasma assisted chemical vapour deposition. *J. Mater. Chem.* **2011**, *21*, 18959–18961. [CrossRef]
60. Fanelli, F.; Mastrangelo, A.M.; Fracassi, F. Aerosol-assisted atmospheric cold plasma deposition and characterization of superhydrophobic organic-inorganic nanocomposite thin films. *Langmuir* **2014**, *30*, 857–865. [CrossRef]

61. Deng, X.; Leys, C.; Vujosevic, D.; Vulksanovic, V.; Cvelbar, U.; De Geyter, N.; Morent, R.; Nikiforov, A. Engineering of composite organosilicon thin films with embedded silver nanoparticles via atmospheric pressure plasma process for antibacterial activity. *Plasma Process. Polym.* **2014**, *11*, 921–930. [CrossRef]
62. Profili, J.; Levasseur, O.; Naudé, N.; Chanec, C.; Stafford, L.; Gherardi, N. Influence of the voltage waveform during nanocomposite layer deposition by aerosol-assisted atmospheric pressure Townsend discharge. *J. Appl. Phys.* **2016**, *120*, 053302. [CrossRef]
63. Liguori, A.; Traldi, E.; Toccaceli, E.; Laurita, R.; Pollicino, A.; Focarete, M.L.; Colombo, V.; Gherardi, M. Co-deposition of plasma-polymerized polyacrylic acid and silver nanoparticles for the production of nanocomposite coatings using a non-equilibrium atmospheric pressure plasma jet. *Plasma Process. Polym.* **2016**, *13*, 623–632. [CrossRef]
64. Brunet, P.; Rincon, R.; Martinez, J.; Matouk, Z.; Fanelli, F.; Chaker, M.; Massines, F. Control of composite thin film made in an Ar/isopropanol/TiO_2 nanoparticles dielectric barrier discharge by the excitation frequency. *Plasma Process. Polym.* **2017**, *14*, e1700049. [CrossRef]
65. Lo Porto, C.; Palumbo, F.; Palazzo, G.; Favia, P. Direct plasma synthesis of nano-capsules loaded with antibiotics. *Polym. Chem.* **2017**, *8*, 1746–1749. [CrossRef]
66. Chemin, J.-B.; Bulou, S.; Baba, K.; Fontaine, C.; Sindzingre, T.; Boscher, N.D.; Choquet, P. Transparent anti-fogging and self-cleaning TiO_2/SiO_2 thin films on polymer substrates using atmospheric plasma. *Sci. Rep.* **2018**, *8*, 9603. [CrossRef] [PubMed]
67. Anagri, A.; Baitukha, A.; Debiemme-Chouvy, C.; Lucas, I.T.; Puplpytel, J.; Tran, T.T.M.; Tabibian, S.; Arefi-Khonsari, F. Nanocomposite coating based on graphene and siloxane polymers deposited by atmospheric pressure plasma. Application to corrosion protection of steel. *Surf. Coat. Technol.* **2019**, *377*, 124928. [CrossRef]
68. Fanelli, F.; Fracassi, F. Aerosol-assisted atmospheric pressure cold plasma deposition of organic-inorganic nanocomposite coatings. *Plasma Chem. Plasma Process.* **2014**, *34*, 473–487. [CrossRef]
69. Stancampiano, A.; Gallingani, T.; Gherardi, M.; Machala, Z.; Maguire, P.; Colombo, V.; Pouvesle, J.-M.; Robert, E. Plasma and aerosols: Challenges, opportunities and perspectives. *Appl. Sci.* **2019**, *9*, 3861. [CrossRef]
70. Lo Porto, C.; Palumbo, F.; Treglia, A.; Camporeale, G.; Favia, P. Aerosol assisted atmospheric pressure PE-CVD of drug containing nano-capsules. *Jpn. J. Appl. Phys.* **2020**, *59*, SA0801. [CrossRef]
71. Fricke, K.; Steffen, H.; von Woedtke, T.; Schroder, K.; Weltmann, K.-D. High rate etching of polymers by means of an atmospheric pressure plasma jet. *Plasma Process. Polym.* **2011**, *8*, 51–58. [CrossRef]
72. Williams, T.S.; Hicks, R.F. Aging mechanism of the native oxide on silicon (100) following atmospheric oxygen plasma cleaning. *J. Vac. Sci. Technol. A* **2011**, *29*, 041403. [CrossRef]
73. Szili, E.J.; Al-Bataineh, S.A.; Bryant, P.M.; Short, R.D.; Bradley, J.W.; Steele, D.A. Controlling the spatial distribution of polymer surface treatment using atmospheric-pressure microplasma jets. *Plasma Process. Polym.* **2011**, *8*, 38–50. [CrossRef]
74. Pavlinak, D.; Galmiz, O.; Pavlinakova, V.; Polacek, P.; Kelar, J.; Stupavska, M.; Cernak, M. Application of dielectric barrier plasma treatment in the nanofiber processing. *Mater. Today Commun.* **2018**, *16*, 330–338. [CrossRef]
75. Galmiz, O.; Pavlinak, D.; Zemanek, M.; Brablec, A.; Cernak, M. Hydrophilization of outer and inner surfaces of poly(vinyl chloride) tubes using surface dielectric barrier discharges generated in ambient air plasma. *Plasma Process. Polym.* **2017**, *14*, e1600220. [CrossRef]
76. Profili, J.; Levasseur, O.; Koronai, A.; Stafford, L.; Gherardi, N. Deposition of nanocomposite coatings on wood using cold discharges at atmospheric pressure. *Surf. Coat. Technol.* **2017**, *309*, 729–737. [CrossRef]
77. Mariotti, D.; Patel, J.; Svrcek, V.; Maguire, P. Plasma-liquid interactions at atmospheric pressure for nanomaterials synthesis and surface engineering. *Plasma Process. Polym.* **2012**, *9*, 1074–1085. [CrossRef]
78. Fabiani, D.; Zaccaria, M.; Focarete, M.L.; Gualandi, C.; Colombo, V.; Ghedini, E.; Gherardi, M.; Laurita, R.; Sanibondi, P. Plasma assisted nanoparticle dispersion in polymeric solutions for the production of electrospun lithium battery separators. In Proceedings of the 2013 IEEE International Conference on Solid Dielectrics (ICSD), Bologna, Italy, 30 June–4 July 2013; pp. 718–721. [CrossRef]
79. Fasano, V.; Laurita, R.; Moffa, M.; Gualandi, C.; Colombo, V.; Gherardi, M.; Zussman, E.; Vasilyev, G.; Persano, L.; Camposeo, A.; et al. Enhanced electrospinning of active organic fibers by plasma treatment on conjugated polymer solutions. *ACS Appl. Mater. Interfaces* **2020**, *12*, 26320–26329. [CrossRef] [PubMed]
80. Boscher, N.D.; Duday, D.; Heier, P.; Heinze, K.; Hilt, F.; Choquet, P. Plasma polymer membranes for immobilising metalloporphyrins. *Plasma Process. Polym.* **2013**, *10*, 336–344. [CrossRef]
81. Nwankire, C.E.; Ardhaoui, M.; Dowling, D.P. The effect of plasma-polymerised silicon hydride-rich polyhydrogenmethylsiloxane on the adhesion of silicone elastomers. *Polym. Int.* **2009**, *58*, 996–1001. [CrossRef]
82. Stallard, C.P.; Iqbal, M.M.; Turner, M.M.; Dowling, D.P. Investigation of the formation mechanism of aligned nano-structured siloxane coatings deposited using an atmospheric plasma jet. *Plasma Process. Polym.* **2013**, *10*, 888–903. [CrossRef]
83. Peng, T.; Pulpytel, J.; Horovitz, I.; Jaiswal, A.K.; Avisar, D.; Mamane, H.; Lalman, J.A.; Arefi-Khonsari, F. One-step deposition of nano-Ag-TiO_2 coatings by atmospheric pressure plasma jet for water treatment: Application to trace pharmaceutical removal using solar photocatalysis. *Plasma Process. Polym.* **2019**, *16*, 1800213. [CrossRef]
84. Rapp, C.; Baumgartel, A.; Artmann, L.; Eblenkamp, M.; Asad, S.S. Open air plasma deposited antimicrobial SiO_x/TiO_x composite films for biomedical applications. *Curr. Dir. Biomed. Eng.* **2016**, *2*, 43–47. [CrossRef]
85. Korzec, D.; Nettesheim, S. Application of a pulsed atmospheric arc plasma jet for low-density polyethylene coating. *Plasma Process. Polym.* **2020**, *17*, e1900098. [CrossRef]

86. Kuchakova, I.; Ionita, M.D.; Ionita, E.R.; Lazea-Stoyanova, A.; Brajnicov, S.; Mitu, B.; Dinescu, G.; De Vrieze, M.; Cvelbar, U.; Zille, A.; et al. Atmospheric pressure plasma deposition of organosilicon thin films by direct current and radio-frequency plasma jets. *Materials* **2020**, *13*, 1296. [CrossRef]
87. Homola, T.; Matousek, J.; Hergelova, B.; Kormunda, M.; Wu, L.Y.L.; Cernak, M. Activation of poly(methyl methacrylate) surfaces by atmospheric pressure plasma. *Polym. Degrad. Stab.* **2012**, *97*, 886–892. [CrossRef]
88. Dimitrakellis, P.; Patsidis, A.C.; Smyrnakis, A.; Psarras, G.C.; Gogolides, E. Atmospheric plasma nanotexturing of organic-inorganic nanocomposite coatings for multifunctional surface fabrication. *ACS Appl. Nano Mater.* **2019**, *2*, 2969–2978. [CrossRef]
89. Fanelli, F.; Fracassi, F.; d'Agostino, R. Deposition and etching of fluorocarbon thin films in atmospheric pressure DBDs fed with Ar–CF_4–H_2 and Ar–CF_4–O_2 mixtures. *Surf. Coat. Technol.* **2010**, *204*, 1779–1784. [CrossRef]
90. Ibrahim, J.; Al-Bataineh, S.A.; Michelmore, A.; Whittle, J.D. Atmospheric pressure dielectric barrier discharges for the deposition of organic plasma polymer coatings for biomedical application. *Plasma Chem. Plasma Process.* **2021**, *41*, 47–83. [CrossRef]
91. Alexandrov, S.E.; Tyurikov, K.S.; Kirilenko, D.A.; Redkov, A.V.; Lipovskii, A.A. Low-temperature atmospheric pressure plasma-enhanced CVD of nanocomposite coatings "molybdenum disulfide (filler)–silicon oxide (matrix)". *Adv. Mater. Interfaces* **2017**, *4*, 1700241. [CrossRef]
92. Pulpytel, J.; Kumar, V.; Peng, P.; Micheli, V.; Laidani, N.; Arefi-Khonsari, F. Deposition of organosilicon coatings by a non-equilibrium atmospheric pressure plasma jet: Design, analysis and macroscopic scaling law of the process. *Plasma Process. Polym.* **2011**, *8*, 664–675. [CrossRef]
93. Carton, O.; Ben Salem, D.; Pulpytel, J.; Arefi-Khonsari, F. Improvement of the water stability of plasma polymerized acrylic acid/MBA coatings deposited by atmospheric pressure air plasma jet. *Plasma Chem. Plasma Proc.* **2015**, *35*, 819–829. [CrossRef]
94. Hsu, Y.W.; Yang, Y.-J.; Wu, C.-Y.; Hsu, C.-C. Downstream characterization of an atmospheric pressure pulsed arc jet. *Plasma Chem. Plasma Process.* **2010**, *30*, 363–372. [CrossRef]
95. Chang, K.M.; Ho, P.-C.; Ariyarit, A.; Yang, K.H.; Hsu, J.-M.; Wu, A.-J.; Chang, C.-C. Enhancement of the light-scattering ability of Ga-doped ZnO thin films using SiO_x nano-films prepared by atmospheric pressure plasma deposition system. *Thin Solid Films* **2013**, *549*, 460–464. [CrossRef]
96. Brès, L.; Sanchot, A.; Rives, B.; Gherardi, N.; Naudé, N.; Aufray, M. Fine-tuning of chemical and physical polymer surface modifications by atmospheric pressure post-discharge plasma and its correlation with adhesion improvement. *Surf. Coat. Technol.* **2019**, *362*, 388–396. [CrossRef]
97. Brés, L.; Gherardi, N.; Naudé, N.; Rives, B. Experimental investigations of a remote atmospheric pressure plasma by electrical diagnostics and related effects on polymer composite surfaces. *Eur. Phys. J. Appl. Phys.* **2021**, *95*, 30801. [CrossRef]
98. Favaro, M.; Patelli, A.; Ceccato, R.; Dirè, S.; Callone, E.; Fredi, G.; Quaranta, A. Thin films of plasma-polymerized n-hexane and ZnO nanoparticles co-deposited via atmospheric pressure plasma jet. *Coatings* **2021**, *11*, 167. [CrossRef]
99. Zuber, B.K.; Murphy, P.; Evans, D. One-step fabrication of nanocomposite thin films of PTFE in SiO_x for repelling water. *Adv. Eng. Mater.* **2014**, *17*, 474–482. [CrossRef]
100. Schütze, A.; Jeong, J.Y.; Babayan, S.E.; Park, J.; Selwyn, G.S.; Hicks, R.F. The atmospheric pressure plasma jet: A review and comparison to other plasma sources. *IEEE Trans. Plasma Sci.* **1998**, *26*, 1685–1694. [CrossRef]
101. Belmonte, T.; Gries, T.; Cardoso, R.P.; Arnoult, G.; Kosior, F.; Henrion, G. Chemical vapour deposition enhanced by atmospheric microwave plasmas: A large-scale industrial process or the next nanomanufacturing tool? *Plasma Sources Sci. Technol.* **2011**, *20*, 024004. [CrossRef]
102. Lee, S.W.; Liang, D.; Gao, X.P.A.; Sankaran, R.M. Direct writing of metal nanoparticles by localized plasma electrochemical reduction of metal cations in polymer films. *Adv. Funct. Mater.* **2011**, *21*, 2155–2161. [CrossRef]
103. Lee, S.W.; Kumpfer, J.R.; Lin, P.A.; Li, G.; Gao, X.P.A.; Rowan, S.J.; Sankaran, R.M. In situ formation of metal nanoparticle composites via "soft" plasma electrochemical reduction of metallosupramolecular polymer films. *Macromolecules* **2012**, *45*, 8201–8210. [CrossRef]
104. Liu, Y.; Sun, D.; Askari, S.; Patel, J.; Macias-Montero, M.; Mitra, S.; Zhang, R.; Lin, W.; Mariotti, D.; Maguire, P. Enhanced dispersion of TiO_2 nanoparticles in a TiO_2/PEDOT:PSS hybrid nanocomposite via plasma-liquid interactions. *Sci. Rep.* **2015**, *5*, 15765. [CrossRef]
105. Sun, D.; Turner, J.; Jiang, N.; Zhu, S.; Zhang, L.; Falzon, B.G.; McCoy, C.P.; Maguire, P.; Mariotti, D.; Sun, D. Atmospheric pressure microplasma for antibacterial silver nanoparticle/chitosan nanocomposites with tailored properties. *Compos. Sci. Technol.* **2020**, *186*, 107911. [CrossRef]
106. Shelemin, A.; Choukourov, A.; Kousal, J.; Slavinska, D.; Biederman, H. Nitrogen-doped TiO_2 nanoparticles and their composites with plasma polymer as deposited by atmospheric pressure DBD. *Plasma Process. Polym.* **2014**, *11*, 864–877. [CrossRef]
107. Hubert, J.; Mertens, J.; Dufour, T.; Vandencasteele, N.; Reniers, F.; Viville, P.; Lazzaroni, R.; Raes, M.; Terryn, H. Synthesis and texturization processes of (super)-hydrophobic fluorinated surfaces by atmospheric plasma. *J. Mater. Res.* **2015**, *30*, 3177–3191. [CrossRef]
108. Mertens, J.; Hubert, J.; Vandencasteele, N.; Raes, M.; Terryn, H.; Reniers, F. Chemical and physical effect of SiO_2 and TiO_2 nanoparticles on highly hydrophobic fluorocarbon hybrid coatings synthesized by atmospheric plasma. *Surf. Coat. Technol.* **2017**, *315*, 274–282. [CrossRef]

109. Beggio, A.; Fantin, M.; Scopece, P.; Surpi, A.; Patelli, A.; Benedetti, A.; Cristofori, D.; Enrichi, F. Incorporation of Eu-Tb codoped nanophosphors in silica-based coatings assisted by atmospheric pressure plasma jet technology. *Thin Solid Films* **2015**, *578*, 38–44. [CrossRef]
110. Deng, X.; Nikiforov, A.Y.; Coenye, T.; Cools, P.; Aziz, G.; Morent, R.; De Geyter, N.; Leys, C. Antimicrobial nano-silver non-woven polyethylene terephthalate fabric via an atmospheric pressure plasma deposition process. *Sci. Rep.* **2015**, *5*, 10138. [CrossRef]
111. Deng, X.; Nikiforov, A.; Vujosevic, D.; Vuksanovic, V.; Mugosa, B.; Cvelbar, U.; De Geyter, N.; Morent, R.; Leyse, C. Antibacterial activity of nano-silver non-woven fabric prepared by atmospheric pressure plasma deposition. *Mater. Lett.* **2015**, *149*, 95–99. [CrossRef]
112. Nikiforov, A.Y.; Deng, X.; Onyshchenko, I.; Vujosevic, D.; Vuksanovic, V.; Cvelbar, U.; De Geyter, N.; Morent, R.; Leys, C. Atmospheric pressure plasma deposition of antimicrobial coatings of non-woven textiles. *Eur. Phys. J. Appl. Phys.* **2016**, *75*, 24710. [CrossRef]
113. Kratochvil, J.; Kuzminova, A.; Kylian, O. State-of-the-art, and perspectives of, silver-plasma polymer antibacterial nanocomposites. *Antibiotics* **2018**, *7*, 78. [CrossRef]
114. Hou, X.; Choy, K.-L.; Brun, N.; Serin, V. Nanocomposite coatings codeposited with nanoparticles using aerosol-assisted chemical vapour deposition. *J. Nanomater.* **2013**, *2013*, 219039. [CrossRef]
115. Marchand, P.; Hassan, I.A.; Parkin, I.P.; Carmalt, C.J. Aerosol-assisted delivery of precursors for chemical vapour deposition: Expanding the scope of CVD for materials fabrication. *Dalton Trans.* **2013**, *42*, 9406. [CrossRef]
116. Palgrave, R.G.; Parkin, I.P. Aerosol assisted chemical vapor deposition using nanoparticle precursors: A route to nanocomposite thin films. *J. Am. Chem. Soc.* **2006**, *128*, 1587–1597. [CrossRef] [PubMed]
117. Ross, A.D.; Gleason, K.K. The CVD of nanocomposites fabricated via ultrasonic atomization. *Chem. Vap. Depos.* **2006**, *12*, 225–230. [CrossRef]
118. Castaneda-Montes, I.; Ritchie, A.W.; Badyal, J.P.S. Atomised spray plasma deposition of hierarchical superhydrophobic nanocomposite surfaces. *Colloids Surf. A Physicochem. Eng. Asp.* **2018**, *558*, 192–199. [CrossRef]
119. Boscher, N.D.; Obaton, A.; Choquet, P.; Duday, D. Liquid-assisted plasma-enhanced chemical vapor deposition of α-cyclodextrin/PDMS composite thin film for the preparation of interferometric sensors—Application to the detection of benzene in water. *J. Nanosci. Nanotechnol.* **2016**, *16*, 10097–10103. [CrossRef]
120. Ward, L.J.; Schofield, W.C.E.; Baydal, J.P.S.; Goodwin, A.J.; Merlin, P.J. Atmospheric pressure plasma deposition of structurally well-defined polyacrylic acid films. *Chem. Mater.* **2003**, *15*, 1466–1469. [CrossRef]
121. Steele, A.; Bayer, I.; Loth, E. Inherently superoleophobic nanocomposite coatings by spray atomization. *Nano Lett.* **2009**, *9*, 501–505. [CrossRef]
122. Boissiere, C.; Grosso, D.; Chaumonnot, A.; Nicole, L.; Sanchez, C. Aerosol route to functional nanostructured inorganic and hybrid porous materials. *Adv. Mater.* **2011**, *23*, 599–623. [CrossRef] [PubMed]
123. Crick, C.R.; Bear, J.C.; Southern, P.; Parkin, I.P. A General method for the incorporation of nanoparticles into superhydrophobic films by aerosol assisted chemical vapour deposition. *J. Mater. Chem. A* **2013**, *1*, 4336–4344. [CrossRef]
124. Fanelli, F.; Mastrangelo, A.M.; Caputo, G.; Fracassi, F. Tuning the structure and wetting properties of organic-inorganic nanocomposite coatings prepared by aerosol-assisted atmospheric pressure cold plasma deposition. *Surf. Coat. Technol.* **2019**, *358*, 67–75. [CrossRef]
125. Uricchio, A.; Nadal, E.; Plujat, B.; Massines, F.; Plantard, G.; Fanelli, F. Low-temperature atmospheric pressure plasma deposition of TiO_2-based nanocomposite coatings on open-cell polymer foams for photocatalytic water treatment. *Appl. Surf. Sci.* **2021**, *561*, 150014. [CrossRef]
126. Fanelli, F.; Mastrangelo, A.M.; De Vietro, N.; Fracassi, F. Preparation of multifunctional superhydrophobic nanocomposite coatings by aerosol-assisted atmospheric cold plasma deposition. *Nanosci. Nanotechnol. Lett.* **2015**, *7*, 84–88. [CrossRef]
127. Brunet, P.; Rincon, R.; Margot, J.; Matouk, Z.; Massines, F.; Chaker, M. Deposition of homogeneous carbon-TiO_2 composites by atmospheric pressure DBD. *Plasma Process. Polym.* **2017**, *14*, e1600075. [CrossRef]
128. Brunet, P.; Rincon, R.; Matouk, Z.; Chaker, M.; Massines, F. Tailored waveform of dielectric barrier discharge to control composite thin film morphology. *Langmuir* **2018**, *34*, 1865–1872. [CrossRef]
129. Milaniak, N.; Laroche, G.; Massines, F. Atmospheric-pressure plasma-enhanced chemical vapor deposition of nanocomposite thin films from ethyl lactate and silica nanoparticles. *Plasma Process. Polym.* **2021**, *18*, e2000153. [CrossRef]
130. Profili, J.; Levasseur, O.; Blaisot, J.; Koronai, A.; Stafford, L.; Gherardi, N. Nebulization of nanocolloidal suspensions for the growth of nanocomposite coatings in dielectric barrier discharges. *Plasma Process. Polym.* **2016**, *13*, 981–989. [CrossRef]
131. Profili, J.; Dap, S.; Levasseur, O.; Naudé, N.; Belinger, A.; Stafford, L.; Gherardi, N. Interaction of atomized colloid with an ac electric field in a dielectric barrier discharge reactor used for deposition of nanocomposite coatings. *J. Appl. Phys.* **2017**, *50*, 075201. [CrossRef]
132. Chen, X.; Lo Porto, C.; Chen, Z.; Merenda, A.; Allioux, F.; d'Agostino, R.; Magniez, K.; Dai, X.J.; Palumbo, F.; Dumee, L.F. Single step synthesis of Janus nano-composite membranes by atmospheric aerosol plasma polymerization for solvents separation. *Sci. Total Environ.* **2018**, *645*, 22–33. [CrossRef]
133. Matouk, Z.; Torriss, B.; Rincon, R.; Mirzaei, A.; Margot, J.; Chaker, M. Atmospheric plasma dielectric barrier discharge: A simple route to produce superhydrophilic TiO_2@carbon nanostructure. *Plasma Process. Polym.* **2021**, *18*, e2000173. [CrossRef]
134. Deng, X.; Nikiforov, A.; Leys, C. Deposition of antibacterial nanocomposite film using and atmospheric pressure nonequilibrium plasma jet. In Proceedings of the 2014 IEEE 41st International Conference on Plasma Sciences Held with 2014 IEEE International Conference on High-Power Particle Beams, Washington, DC, USA, 25–29 May 2014; pp. 1–4. [CrossRef]

135. Tyurikov, K.S.; Alexandrov, S.; Iankevich, G. Corona discharge plasma application for the deposition of nanocomposite coatings. *Mater. Today Proc.* **2020**, *30*, 403–407. [CrossRef]
136. Jnido, G.; Ohms, G.; Viol, W. One-step deposition of polyester/TiO_2 coatings by atmospheric pressure plasma jet on wood surfaces for UV and moisture protection. *Coatings* **2020**, *10*, 184. [CrossRef]
137. Wallenhorst, L.M.; Dahle, S.; Militz, H.; Ohms, G.; Viol, W. Characterisation of PMMA/ATH layers realised by means of atmospheric pressure plasma powder deposition. *Adv. Condens. Matter. Phys.* **2015**, *2015*, 980482. [CrossRef]
138. Lo Porto, C.; Palumbo, F.; Fracassi, F.; Barucca, G.; Favia, P. On the formation of nanocapsules in aerosol-assisted atmospheric-pressure plasma. *Plasma Process. Polym.* **2019**, *16*, 1900116. [CrossRef]
139. Nadal, E.; Milaniak, N.; Glenat, H.; Laroche, G.; Massines, F. A new approach for synthesizing plasmonic polymer nanocomposite thin films by combining a gold salt aerosol and an atmospheric pressure low-temperature plasma. *Nanotechnology* **2021**, *32*, 175601. [CrossRef] [PubMed]
140. Wang, L.; Lo Porto, C.; Palumbo, F.; Modic, M.; Cvelbar, U.; Ghobeira, R.; De Geyter, N.; De Vrieze, M.; Kos, S.; Sersa, G.; et al. Synthesis of antibacterial composite coating containing nanocapsules in an atmospheric pressure plasma. *Mater. Sci. Eng. C* **2021**, *119*, 111496. [CrossRef] [PubMed]
141. Heyse, P.; Roeffaers, M.B.J.; Paulussen, S.; Hofkens, J.; Jacobs, P.A.; Sels, B.F. Protein immobilization using atmospheric-pressure dielectric-barrier discharges: A route to a straightforward manufacture of bioactive films. *Plasma Process. Polym.* **2008**, *5*, 186–191. [CrossRef]
142. Heyse, P.; Hoeck, A.V.; Roeffaers, M.B.J.; Raffin, J.P.; Steinbuchel, A.; Stoveken, T.; Lammertyn, J.; Verboven, P.; Jacobs, P.A.; Hofkens, J.; et al. Exploration of atmospheric pressure plasma nanofilm technology for straightforward bio-active coating deposition: Enzymes, plasmas and polymers, an elegant synergy. *Plasma Process. Polym.* **2011**, *8*, 965–974. [CrossRef]
143. Da Ponte, G.; Sardella, E.; Fanelli, F.; Paulussen, S.; Favia, P. Atmospheric pressure plasma deposition of poly lactic acid-like coatings with embedded elastin. *Plasma Process. Polym.* **2014**, *11*, 345–352. [CrossRef]
144. Palumbo, F.; Camporeale, G.; Yang, Y.-W.; Wu, J.-S.; Sardella, E.; Dilecce, G.; Calvano, C.D.; Quintieri, L.; Caputo, L.; Baruzzi, F.; et al. Direct plasma deposition of lysozyme-embedded bio-composite thin films. *Plasma Process. Polym.* **2015**, *12*, 1302–1310. [CrossRef]
145. Hsiao, C.-P.; Wu, C.-C.; Liu, Y.-L.; Yang, Y.-W.; Cheng, Y.-C.; Palumbo, F.; Camporeale, G.; Favia, P.; Wu, J.-S. Aerosol-assisted plasma deposition of biocomposite coatings: Investigation of processing conditions on coating properties. *IEEE Trans. Plasma Sci.* **2016**, *44*, 3091–3098. [CrossRef]
146. Cheng, Y.-C.; Hsiao, C.-P.; Liu, Y.-H.; Yang, C.-H.; Chiang, C.-Y.; Lin, T.-R.; Yang, Y.-W.; Wu, J.-S. Enhancing adhesion and polymerization of lipase-plasma-polymerized-ethylene coatings deposited with planar dielectric-barrier-discharge-type aerosol-assisted atmospheric-pressure plasma system. *Plasma Process. Polym.* **2018**, *15*, e1700173. [CrossRef]
147. Amorosi, C.; Ball, V.; Bour, J.; Bertani, P.; Toniazzo, V.; Ruch, D.; Averous, L.; Michel, M. One step preparation of plasma based polymer films for drug release. *Mater. Sci. Eng.* **2012**, *32*, 2103–2108. [CrossRef] [PubMed]
148. Palumbo, F.; Treglia, A.; Lo Porto, C.; Fracassi, F.; Baruzzi, F.; Frache, G.; El Assad, D.; Pistillo, B.C.; Favia, P. Plasma-deposited nanocapsules containing coatings for drug delivery applications. *ACS Appl. Mater. Interfaces* **2018**, *10*, 35516–35525. [CrossRef] [PubMed]
149. Lo Porto, C.; Palumbo, F.; Buxadera-Palomero, J.; Canal, C.; Jelinek, P.; Zajickova, L.; Favia, P. On the plasma deposition of vancomycin-containing nano-capsules for drug-delivery applications. *Plasma Process. Polym.* **2018**, *15*, e1700232. [CrossRef]
150. Morand, G.; Chevallier, P.; Guyon, C.; Tatoulian, M.; Mantovani, D. In-situ one-step direct loading of agents in poly(acrylic acid) coating deposited by aerosol-assisted open-air plasma. *Polymers* **2021**, *13*, 1931. [CrossRef]
151. Beier, O.; Pfuch, A.; Horn, K.; Weisser, J.; Scnabelrauch, M.; Schimanski, A. Low temperature deposition of antibacterially active silicon oxide layers containing silver nanoparticles, prepared by atmospheric pressure plasma chemical vapor deposition. *Plasma Process. Polym.* **2013**, *10*, 77–87. [CrossRef]
152. Spange, S.; Pfuch, A.; Wiegand, C.; Beier, O.; Hipler, U.C.; Grunler, B. Atmospheric pressure plasma CVD as a tool to functionalise wound dressings. *J. Mater. Sci. Mater. Med.* **2015**, *26*, 76. [CrossRef] [PubMed]
153. Jager, E.; Schmidt, J.; Pfuch, A.; Spange, S.; Beier, O.; Jager, N.; Jantschner, O.; Daniel, R.; Mitterer, C. Antibacterial silicon oxide thin films doped with zinc and copper grown by atmospheric pressure plasma chemical vapor deposition. *Nanomaterials* **2019**, *9*, 255. [CrossRef]
154. Lapenna, A.; Fanelli, F.; Fracassi, F.; Armenise, V.; Angarano, V.; Palazzo, G.; Mallardi, A. Direct exposure of dry enzymes to atmospheric pressure non-equilibrium plasmas: The case of tyrosinase. *Materials* **2020**, *13*, 2181. [CrossRef]
155. Fracassi, F.; d'Agostino, R.; Palumbo, F.; Angelini, E.; Grassini, S.; Rosalbino, F. Application of plasma deposited organosilicon thin films for the corrosion protection of metals. *Surf. Coat. Technol.* **2003**, *174–175*, 107–111. [CrossRef]
156. De Freitas, A.S.M.; Maciel, C.C.; Rodrigues, J.S.; Ribeiro, R.P.; Delgado-Silva, A.O.; Rangel, E.C. Organosilicon films deposited in low-pressure plasma from hexamethyldisiloxane—A review. *Vacuum* **2021**, *194*, 110556. [CrossRef]
157. Angelini, E.; Grassini, S.; Ingo, G.M.; Mombello, D.; Fracassi, F.; Palumbo, F. Surface analysis of SiO_2-like high-barrier thin films for protection of silver artefacts. *Surf. Interface Anal.* **2010**, *42*, 666–670. [CrossRef]
158. Lommatzsch, U.; Ihde, J. Plasma polymerization of HMDSO with an atmospheric pressure plasma jet for corrosion protection of aluminum and low-adhesion surfaces. *Plasma Process. Polym.* **2009**, *6*, 642–648. [CrossRef]

159. Regula, C.; Lukasczyk, T.; Ihde, J.; Fladung, T.; Wilken, R. Corrosion protection of metal surfaces by atmospheric pressure plasma jet treatment. *Progr. Org. Coat.* **2012**, *74*, 734–738. [CrossRef]
160. Aparicio, F.J.; Borras, A.; Blaszczyk-Lezak, I.; Gröning, P.; Álvarez-Herrero, A.; Fernández-Rodríguez, M.; González-Elipe, A.R.; Barranco, A. Luminescent and optical properties of nanocomposite thin films deposited by remote plasma polymerization of rhodamine 6G. *Plasma Process. Polym.* **2009**, *6*, 17–26. [CrossRef]
161. Faupel, F.; Zaporojtchenko, V.; Strunskus, T.; Elbahri, M. Metal-polymer nanocomposites for functional applications. *Adv. Eng. Mater.* **2010**, *12*, 1177–1190. [CrossRef]
162. Biederman, H.; Kylian, O.; Drabik, M.; Choukourov, A.; Polonskyi, O.; Solar, P. Nanocomposite and nanostructured films with plasma polymer matrix. *Surf. Coat. Technol.* **2012**, *211*, 127–137. [CrossRef]
163. Kylìan, O.; Polonskyi, O.; Kratochvil, J.; Artemenko, A.; Chokourov, A.; Drabik, M.; Solar, P.; Slavinska, D.; Biederman, H. Control of wettability of plasma polymers by application of Ti nano-clusters. *Plasma Process. Polym.* **2012**, *9*, 180–187. [CrossRef]
164. Kylian, O.; Petr, M.; Serov, A.; Solar, P.; Polonskyi, O.; Hanus, J.; Chokourov, A.; Biederman, H. Hydrophobic and superhydrophobic coatings based on nanoparticles overcoated by fluorocarbon plasma polymer. *Vacuum* **2014**, *100*, 57–60. [CrossRef]
165. Ellinas, K.; Dimitrakellis, P.; Sarkiris, P.; Gogolides, E. A Review of fabrication methods, properties and applications of superhydrophobic metals. *Processes* **2021**, *9*, 666. [CrossRef]